July 2020

Processes, Patterns, and Predictions of Soil Moisture Variation in Upland and Peatland Cranberry Farms in Massachusetts

Rebecca Brennan
University of Massachusetts Amherst

PROCESSES, PATTERNS, AND PREDICTIONS OF SOIL MOISTURE VARIATION IN UPLAND AND PEATLAND CRANBERRY FARMS IN MASSACHUSETTS

A Thesis Presented

By

REBECCA BRENNAN

Submitted to the Graduate School of the
University of Massachusetts Amherst in partial fulfillment
of the requirements for the degree of

MASTER OF SCIENCE

May 2020

Plant Biology

PROCESSES, PATTERNS, AND PREDICTIONS OF SOIL MOISTURE VARIATION IN UPLAND AND PEATLAND CRANBERRY FARMS IN MASSACHUSETTS

A Thesis Presented

By

REBECCA BRENNAN

Approved as to style and content by:

_____
Hilary A. Sandler, Chair

_____
Casey Kennedy, Member

_____
Michelle DaCosta, Member

_____
Peter Jeranyama, Member

_____
Samuel Hazen, Program Director
Plant Biology

ACKNOWLEDGMENTS

The completion of this thesis would not have been possible without the incredible commitment of several people:

Hilary Sandler and Casey Kennedy for providing advice and mentorship through the completion of my project, reinvigorating my love for science, and encouraging me to embrace change and contingency plans.

My committee member, Michelle DaCosta, for her excellent guidance towards a nuanced understanding of plant physiology and stress response.

Peter Jeranyama, another committee member, who helped me to begin my research and gain an excellent understanding of plant physiology.

Every member of the UMass Cranberry Station, who made me a part of their community and supported me through every step and question.

And, finally, my family, whose support means everything.

ABSTRACT

PROCESSES, PATTERNS, AND PREDICTIONS OF SOIL MOISTURE VARIATION IN UPLAND AND PEATLAND CRANBERRY FARMS IN MASSACHUSETTS

MAY 2020

REBECCA BRENNAN, B.S., UNIVERSITY OF DELAWARE

M.S., UNIVERSITY OF MASSACHUSETTS AMHERST

Directed by: Dr. Hilary A. Sandler

The American Cranberry (*Vaccinium macrocarpon* Ait.) represents a vital sector of the economy of southeastern Massachusetts. Due to the hydrogeological and edaphic characteristics of peatlands, variations in soil drainage and soil moisture represent major management challenges for growers in Massachusetts. An emerging trend of upland (mineral soil) cranberry farms planted with new hybrid cultivars has the potential to enhance the profitability and long-term viability of cranberry production in Massachusetts. However, sparse data exist on soil moisture characteristics of peatland and upland cranberry farms. The purpose of this research was to elucidate the differences in soil moisture between upland and peatland cranberry farms, to evaluate the soil temperature-moisture relationship and its use for inferring soil moisture, and to explore the use of unmanned aircraft systems (UAS) as a soil moisture management tool in cranberry agriculture. In this thesis, we found that volumetric soil water content (θ_v) in upland farms ranged from 5-15%, contrasting with values of 10-40% for peatland farms. In general, soil moisture in upland farms was two times drier and four times more

uniform than peatlands farms. Our results suggest that open ditches should be dredged to at least 50 cm to obtain irrigation setpoints of -5 to -2 kPa for Massachusetts cranberry farms. We found that soil temperature and near-surface temperature were accurate predictors of soil moisture but were also strongly dependent on the magnitude of differences between air and water temperature. Soil and near-surface temperatures were also better predictors of moisture in soils with lower vegetation coverage and organic matter content. Near-surface temperature collected with a UAS was consistent with field measurements of θ_v, suggesting that UAS could be used to assist Massachusetts cranberry farmers by predicting large-scale variation in θ_v and offering management insights.

TABLE OF CONTENTS

LIST OF TABLES

Table Page

LIST OF FIGURES

Figure Page

CHAPTER 1

INTRODUCTION

1.1 Massachusetts Cranberry Industry

The American cranberry (*Vaccinium macrocarpon* Ait.) is a trailing, non-deciduous vine. When cultivated, cranberry forms a continuous low mat of vegetation. As an obligate wetland plant, cranberry belongs to the *Ericaceae* (heath) family and is most closely related to blueberry and laurel. Cranberry plants, which produce large, dark red fruit, are adapted to the acidic and nutrient-poor conditions in the high latitude peatlands of North America (Gleason and Cronquist, 1991). The name cranberry is believed to originate from “craneberry," owing to its small, white to light pink pedulant blossoms that resemble a crane (Thomas, 1990). Commercial cultivation of cranberry is a relatively recent development in the horticultural history of the plant. Wild cranberry was harvested by the Wampanoag people for over 12,000 years and consumed as a fresh and dried fruit. However, the first recorded attempt to cultivate the plant is credited to Captain Henry Hall, of Dennis MA, in 1816 (Thomas, 1990). Hall began the practice of layering sand on top of cranberry vines and actively transplanting vines into new locations, a practice that began the conversion of most natural peatlands in southeastern Massachusetts to commercial farms (Deubert and Caruso, 1989; Thomas, 1990). Today, cranberries are primarily grown in North America, with ~85% of U.S. cranberries produced by Wisconsin and Massachusetts (B. Wick, pers. comm., 2019).

The cranberry industry is the largest and most valuable food crop produced in Massachusetts (CCCGA, 2019). In 2017, 87 million kg of cranberries were harvested

from 4,568 ha of cranberry farms with a cumulative economic footprint of $59.6 billion (Alston et al., 2014; USDA NASS, 2018). In 2017, Massachusetts accounted for 23% of U.S. production of cranberries (USDA NASS, 2018), which was the second highest of any growing region in the U.S. A recent economic analysis valued the MA cranberry industry at $0.25 billion and credited it with the production of 1,682 direct jobs (Alston et al., 2014). Massachusetts cranberry farms range in size, from 0.4 to 40 ha, with 70% of growers farming less than 8 ha (B. Wick, pers. comm., 2019). Although the industry is principally reliant on processed food products, cranberries have several medicinal benefits related to improved urinary and heart health (Paredes-López et al., 2010; Neto and Vinson, 2011).

1.2 Peatland versus Upland Soils

Massachusetts peatland cranberry farms are cultivated in sand that caps parent soils of bogs or fens that are collectively known as peatlands (Deubert and Caruso, 1989; Thomas, 1990; Craft, 2016; Kennedy et al., 2018). In Massachusetts, peatlands form as partially decomposed plant material accumulates in kettle holes of glacial outwash deposits. Kettle holes are depressions in the landscape that form when large pieces of buried ice are deposited as retreating glaciers melt (Deubert and Caruso, 1989). In many cases, peatlands are isolated from groundwater and fed predominantly by precipitation, thus creating acidic soil conditions that are suitable for cranberry vine growth (Masterson et al., 2009). In addition, peat functions as a water-confining layer that is necessary for flooding, a management tool used by >90% of growers in Massachusetts (Kennedy et al., 2018).

Variation in peat thickness is a landscape feature that influences water management of cranberry production and is an essential consideration when planning farm construction. This irregularity may result in uneven soil drainage, which is influenced in part by groundwater exchanges with the landscape (Hare et al., 2017). Variable groundwater exchanges and uneven soil drainage produce highly heterogeneous soil moisture conditions, which influences photosynthesis, cooling, oxygen absorption, nutrient transport, and plant growth and development (Blatt et al., 2014; Pelletier et al., 2015b; Caron et al., 2017; Hare et al., 2017; Kennedy et al., 2017). Consequently, adequate soil drainage is important for successful commercial cranberry production, with up to 50% of the variance in cranberry yield related to soil drainage (Bulot et al., 2016).

In addition to their management challenges, traditional peatland farms contribute disproportionately to the nitrogen load delivered from cranberry agriculture to coastal discharge areas (Kennedy and Hoekstra, in review). Of particular concern are peatland farms that are located in riparian areas, or what are locally referred to as "flowthrough" farms. In these farms, a channel containing moving water serves as the irrigation and drainage canal (Hoekstra et al., 2020).

Given these management and environmental concerns with peatland farms, construction of upland farms (on mineral soils) over the past few decades has led to these latter farm types now comprising approximately 25% of Massachusetts cranberry acreage (Hoekstra et al., 2020). Construction of upland farms provides an opportunity to replant with hybrid cultivars, such as 'Mullica Queen,' which are capable of nearly twice the fruit production compared with the native varieties 'Early Black' and 'Howes' (Caruso, 2008). Upland farms are typically constructed near lakes or streams, or where dug-out

ponds intercept the regional water table (DeMoranville et al., 2001; Sandler and DeMoranville, 2008). A key characteristic of upland farms is a water-confining layer, which typically consists of low permeability clays capped by organic matter and a layer of sand. This water-confining layer may form a perched water table, an artificial water table held in place above the regional water table depth (DeMoranville et al., 2001; Kennedy et al., 2018).

Peatland farms consist of irregularly shaped pieces (or farm units) that generally follow the natural contours of peat deposits. These farms range in size, from less than 0.4 to 40 ha, with 70% of farms consisting of less than 8 ha (Deubert and Caruso, 1989; B. Wick. pers. comm., 2019). Figure 1 compares aerial views of typical peatland and upland farms. Renovated or newly constructed farms are initially capped by a thick layer of sand. Over time, alternating layers of organic matter and sand develop, creating the "layer cake" patterning observed in established farms (Deubert and Caruso, 1989). This layering may result in localized ponding or uneven drainage. In Massachusetts, upland farms are occasionally referred to as "Wisconsin-style" farms, the majority of which consist of long, rectangular beds planted with high-producing cultivars, in contrast to the irregular shapes that typify peatland farms. Application technology efficiency, management practices, drainage uniformity, the size of farm pieces, and primarily, cultivar selection, contribute to the gap in cranberry production between Massachusetts and Wisconsin. In 2017, Massachusetts farms produced an average of 154 barrels ac^{-1} (1 barrel equals 100 lb) (17,200 kg ha^{-1}) as compared to the Wisconsin average of 259 barrels ac^{-1} (29,000 kg ha^{-1}) (USDA NASS, 2018).

1.3 Soil Moisture Management

Plants absorb water from soil pore spaces, which also store essential plant nutrients such as potassium, nitrogen, and phosphorus. Water within the plant facilitates the transfer of these nutrients, while also providing structural support, driving cell expansion, and regulating photosynthesis (Blatt et al., 2014). During photosynthesis, water is moved from the roots to the leaves where it is exchanged for atmospheric carbon dioxide. Stomatal conductance (g) in cranberry occurs at a rate of 0.2-0.3 mol m^{-2} s^{-1} (Bland et al., 1995; Vanderleest and Bland, 2016). As such, photosynthesis is tightly coupled to evapotranspiration, which is estimated to occur at a rate of 7-17 mm wk^{-1} for cranberry farms in Massachusetts (Hattendorf, 1996; Vanderleest and Bland, 2016; Kennedy et al., 2017). From a plant physiology perspective, soil moisture management is arguably the most critical agricultural management practice.

Since the 1940s, inadequate drainage has been observed in connection with decreased cranberry production (Franklin and Cross, 1948). However, the mechanistic relationships between cranberry production and soil drainage were poorly understood until the 2000s. Research has shown that inadequate drainage adversely affects root growth (Baumann et al., 2005), oxygen level (Pelletier et al., 2016b), photosynthesis (Laurent, 2014), disease pressure (Caruso, 1989), and crop yield (Pelletier et al., 2015a,b; Pelletier et al., 2016b; Caron et al., 2017; Jeranyama et al., 2017; Pelletier et al., 2017). Conversely, dry soil moisture conditions may also affect cranberry yield by impairing thermoregulation and photosynthesis (Caron et al., 2017). Overall, soil water availability outside of an ideal range for plant access immediately impacts stomatal conductance.

Limitations to the exchange of carbon dioxide and oxygen impair a plant's ability to sequester carbon, and therefore reduce net yield and, in the case of cranberry, fruit production.

Soil moisture in cranberry farms may be managed using different strategies. Ditch systems surround (i.e., perimeter ditches) and sometimes run through (i.e., interior ditches) cranberry farms. The water level in ditches may be lowered or raised using a pump or by gravity. The adjustment of ditch height manipulates the water table within the cranberry farm (Jeranyama et al., 2017). The installation of tile drains may facilitate drainage and assist subirrigation. Tile drains are perforated plastic pipes installed to a depth that should be adjusted based upon drainage conditions and water table depth. These perforated pipes allow for water to drain through them, rather than being trapped and creating saturated growing conditions (DeMoranville et al., 2016).

Conventional methods of irrigation application for commercial cranberry farms include overhead irrigation and subirrigation. Overhead irrigation is applied by sprinkler heads (either as impact heads attached to risers or as pop-up heads) that are part of an underground water conveyance system, which is driven by a pump. Overhead irrigation draws water from a local reservoir or well and is typically applied during the morning hours or to supply soil moisture or to mitigate heat or frost damage (Sandler and Heywood, 2010). Subirrigation is provided by elevating the water table and bringing water to cranberry roots from below and through lateral movement. Irrigation by this method may be provided by pumping water into ditches, raising the water table from below, or by pumping water into tile-drainage systems (DeMoranville et al., 2016;

Vanderleest et al., 2016). Soil moisture is often measured as soil water tension (ψ), which is the force exerted by a plant to extract water from the soil. Current recommended irrigation setpoints based on ψ are -2.0 to -5.0 kPa for Massachusetts farms (Jeranyama et al., 2017) and -4.0 to -7.0 kPa for Wisconsin and Canadian farms (Pelletier et al. 2015a,b; Caron et al., 2017). In addition to the use of ψ, soil moisture on cranberry farms is also inferred from water table depth, or the upper surface of soil saturation. Water table depth is monitored by the use of floats installed in shallow wells (Lampinen, 2000). These devices referred to as "water level floats," are one of the least expensive, simplest, and most accurate options to measure soil moisture on farms with sandy soil and water table depths ranging from 15 and 45 cm (Lampinen, 2000). The measurement of gravimetric water content (θ_g) is also an excellent method; however, it is relatively time-intensive compared with standard methods of measuring ψ and θ_v (Bilskie, 2001). Volumetric water content (θ_v) appears to yield variable output for the lower end of the measurement range (Jeranyama et al., 2017), and thus is not widely used by growers.

Many conventional methods of soil moisture measurement are invasive, and some can be quite expensive and time consuming. The evolving discipline of precision agriculture offers solutions to the collection of soil moisture data over large spatial scales. In particular, soil volumetric heat capacity, C_{soil}, which is defined as the quantity of heat that can be stored in soil, can be determined by the sum of heat capacities occupied by the soil's solid, water, and air phases (De Vries, 1963; Robinson et al., 2008)

$$C_{soil} = (\rho c)_s(1-\phi) + (\rho c)_w\theta_v + (\rho c)_a(\phi - \theta_v), \quad (1)$$

where ρ is density, c is specific heat, ϕ is porosity, and θ_v is volumetric water content, and subscripts s, w, and a represent the soil's solid, water, and air phases, respectively. With knowledge of c, ρ, ϕ, estimates of which are generally available in the literature (e.g., Kay and Goit, 1975), C_{soil} is directly proportional to θ_v. Although c does vary with temperature, the effect that temperature has on c is relatively minor (Robinson et al., 2008). Therefore, values of c are essentially constant, and C_{soil} varies as a function of θ_v.

The conceptual framework presented in Eqn. 1 has been applied using satellite, aerial, and ground-based measuring techniques to infer θ_v from estimates of soil temperature at scales ranging from potted plants (cm) to large farms (ha) (Ishimwe et al., 2014; Gago et al., 2015). Early applications of soil temperature to estimate θ_v was undertaken using satellites and microwaves for rangeland, pasture, and winter wheat land areas ranging from 603-740 km^2 (Jackson et al., 1995). However, satellite-based remote sensing provides relatively low resolution, ranging in the 10s to 100s of meters scale (Mulla, 2013). Therefore, this measurement technique is best suited for regional-scale analysis (areas >100 km^2) (Mulla, 2013; Zhang and Zhou, 2016).

The use of unmanned aircraft systems (UAS) is a novel approach to managing soil moisture content in cranberry production. Research shows promise in estimating θ_v from measurements of soil temperature, while also drastically enhancing resolution, from a m to a cm resolution (Zhang and Kovacs, 2012; Ishimwe et al., 2014; Chang and Hsu, 2018). UAS fly below 120 m and can rapidly capture highly accurate images of >10-ha areas in a matter of minutes. For instance, crop water stress and plant water stress have

been rapidly mapped by UAS thermal imaging in vineyards (Bellvert et al., 2014; Santesteban et al., 2017).

Remote sensing techniques have been used in cranberry research (Oudemans et al., 2002; Kerry et al., 2017; Hoekstra et al., 2020). Satellite-scale remote imagery has been used to detect yield loss in cranberry (Oudemans et al., 2002; Kerry et al., 2017). In addition, normalized difference vegetation index (NDVI) has been used to assess how greenness correlates with increased chlorophyll and the health of cranberry (Mallick et al., 2013). Applications for UAS in cranberry are expanding rapidly and may provide researchers and farmers with a means to quickly obtain high-resolution crop information over large scales, from weed pressure to plant water stress to water management (Oudemans et al., 2002; Kerry et al., 2017; Sandler, 2018; Hoekstra et al., 2020).

1.4 Research Objectives

Due to the importance of soil moisture management in cranberry production, as well as the unique hydrogeological characteristics of Massachusetts cranberry farms, the objectives of this thesis were the following:

1. Evaluate processes affecting soil moisture variation between peatland and upland cranberry farms in Massachusetts.
2. Provide specific management recommendations that enhance soil moisture conditions on peatland and upland cranberry farms in Massachusetts.

1.5 Hypotheses

Test flights and on-the-ground recordings indicated an association between soil moisture measurements and thermal image temperature trends. Additionally, farm renovation (the prevalence of upland farms vs. peatland farms) is an emerging trend in Massachusetts. The renovation process and the management of renovated farms may benefit from elucidation of soil moisture patterns and trends. Due to these observations and the increasing prevalence of UAS technology for precision agriculture, our hypotheses were the following:

1. Soil temperature-moisture relationships are correlated and may be used to infer soil moisture on Massachusetts cranberry farms.
2. Peatland and upland Massachusetts cranberry farms differ in their soil moisture patterns and trends.
3. UAS technology may assist Massachusetts cranberry farmers by predicting soil moisture and offering management insights.

CHAPTER 2

SITE SELECTION

2.1 Sites

The study area was located in southeastern Massachusetts, United States. Sites include an established peatland farm, site SB, and an upland farm in three stages of successional growth, site CF. Farm type is classified by the parent soil of the area, with organic soil observed in peatlands, and mineral soil in uplands. The locations selected for this investigation included one 0.7-ha unit of site SB (SB-13), and four 1.2 to 1.6-ha units of site CF (CF-0, CF-1, CF-2, CF-3) (Figure 2). Sites SB and CF differed by cultivar, age (years since planting) and parent soil material (i.e., organic vs. mineral). We classified sites as upland if <30% of the farm was mapped as organic soil (i.e., Freetown or Swansea series) and peatland if organic soils made up >70% of the farm area (Soil Survey Staff, 2019). Both sites have a layer of sand that overlies parent soil. A layer of sand is periodically applied to cranberry farms, following recommended horticultural practices for anchoring runners (Hunsberger et al., 2006). Fertilizer application rates varied according to recommendations provided by the University of Massachusetts Cranberry Station (UMCS) (Ghantous et al., 2018). For both sites, pesticides were applied to control pests, weeds, and disease, and setpoints of -2.0 to -5.0 kPa were used to initiate overhead or subsurface irrigation.

2.2 Peatland Farm

Site SB, which is managed by staff at the UMCS, has been an active experimental farm since 1911. Site SB is located in East Wareham, Massachusetts (41.767N, -70.667W), where 10% of the state's cranberry acreage is farmed (B. Wick, pers. comm., 2019). Site SB consists of four farm units (or sections) that encompass an area of approximately 5 ha. One 0.7-ha section was selected for study, labelled "SB-13". SB-13 (designated as such since vines were planted 13 yr ago) was classified as a peatland farm, based on soils mapped as 45% Freetown, 45% Swansea, and 10% Carver (Soil Survey Staff, 2019). The peat layer begins at approximately 0.5 m below the sand surface, has a mean thickness of 1.6 m, and exhibits a pattern of increasing thickness towards the center of the farm (Kennedy et al., 2018).

In 2006, site SB was renovated, a process that included removing existing vines and replanting new vines, extending the farm area beyond the underlying peat layer towards the edges of the farm, and squaring off the rounded shape of the farm. These expanded edges were classified as Carver soils (Soil Survey Staff, 2019) and potentially lacked the water retention capacity provided by a peat layer. They were consistently observed to be drier than the original sections of the farm based on soil moisture monitoring in 2017 and 2018. The majority of site SB is planted with the cultivar 'Stevens,' currently one of the most widely farmed and researched cranberry cultivars in North America. In Massachusetts, ~25% of all cranberry farm acreage is planted with 'Stevens' vines (M. Sylvia, pers. comm., 2019). 'Stevens' is a result of a hybridization trial crossing 'McFarlin' and 'Potter' cultivars, noted for good keeping quality, early ripening, and intermediate disease resistance (Caruso, 2008).

2.3 Upland Farm

Site CF is located in Carver, Massachusetts (41.825N, -70.703W), where, as of 2011, 24% of the state's cranberry acreage is farmed (B. Wick. pers. comm., 2019). Site CF is composed of a mixture of mineral and organic soils, but the majority (65%) of the farm was mapped as mineral soil series Carver and Tihonet (Soil Survey Staff, 2019). Site CF was constructed to accommodate a boom sprayer, which can deliver precise and uniform applications of fertilizer and pesticides. A perimeter ditch encircles each farm unit; 15-m-wide unvegetated dikes were constructed at the top of a vegetated slope to facilitate vehicle and pedestrian access. Due to sampling constraints, 50-100 m wide sections of each unit were selected for sensor placement and UAS imaging (refer to Figure 2).

Two sections, one unplanted (0 yr) and one established (3 yr), make up two 14-ha units (CF-0 and CF-3, respectively). Another unit was split into two sections: 4 ha with 2-yr vine (CF-2) and 3.2 ha with 1-yr vines (CF-1). CF-3 consists of 45%, 15%, 15%, and 25% Carver, Tihonet, Swansea, and Freetown soils, respectively. CF-1 and CF-2 consist entirely of Carver coarse sand or Carver loamy coarse soil (Soil Survey Staff, 2019). CF-0 includes mineral soils (~70% Carver and Tihonet) and organic soils (~30% Freetown coarse sand and Udipsamment soil) (Soil Survey Staff, 2019). Site CF is considered an upland farm, with all sections planted with 'Grygleski-1' (aka 'GH-1'), developed by its namesake Ed Grygleski by crossing cultivars 'Rezin' and 'Sears' in Wisconsin in 1980. Grown successfully in Wisconsin and New Jersey, the hybrid has recently become a popular choice for Massachusetts renovations due to the cultivar's large fruit size and high yields. Images depicting vine growth at all locations are presented in Figure 3.

CHAPTER 3

MATERIALS AND METHODS

3.1 Materials and Methods

We conducted lab and field measurements to evaluate soil properties, soil moisture, and soil temperature in upland and peatland cranberry farms. Lab experiments were performed under controlled environmental conditions to assess relationships among water depth, gravimetric water content (θ_g), volumetric water content (θ_v), soil moisture tension (ψ), soil temperature (T_{soil}), and near-surface temperature ($T_{surface}$). Field studies consisted of repeated, spatially intensive measurements of θ_g, θ_v, and ψ during the summer of 2019. In addition to traditional field methods, we explored the use of unmanned aerial systems (UAS) fitted with a thermal infrared camera to infer metrics of soil moisture from near-surface temperature ($T_{surface}$). Traditional field methods were used to evaluate the feasibility of UAS thermal imagery as a tool for soil moisture management in large (>4 ha) cranberry farms.

3.2 Growth Chamber Experiments

Intact soil cores were collected from peatland (SB-13), and upland (CF-3 and CF-0) farms. At each location, three random cores were collected from a small (3 m^2) grid that was observed to be representative of average canopy thickness (see Figure 3). To represent a uniform, unvegetated soil core (from a newly prepared planting surface), sand, destined to be used on CF-0, was collected, homogenized, sieved (<1.2 mm), and placed into three PVC pipes (as described below).

To collect cores at SB-13 and CF-3, an 18 cm-diameter, 45-cm long, PVC pipe was carefully inserted to penetrate the plant root zone, taking care to minimize injury to the vines and soil disturbance, then hammered to the soil depth of 40 cm. The surrounding (~15 cm) of vegetation and soil was extracted, and the core was capped at the bottom and removed. A fine-mesh nylon fabric was attached to the bottom of each soil core to prevent soil loss. Cores were transported to the lab within 30 min of collection and placed in the growth chamber set to the mid-range temperature regime for a 48-hr acclimation period (Figure 4). PVC pipes, containing the cores, were marked at depth intervals of 0, 10, 20, 30, and 40 cm below the soil surface.

The three soil cores collected from each site were wetted in a single 27-L plastic tank, which was placed in a plant growth chamber (Percival model E-36VLHO) located at the UMCS (Figure 4). Since the growth chamber could only hold one tank at a time, each location (SB-13, CF-0, and CF-3) was evaluated in a separate run, for a total of three runs. A Mariotte bottle was used to hold a constant water depth of 35 cm from the soil surface for at least 48 hr before experiments were initiated (Engstrom-Heg, 1971). We observed some vine mortality over this initiation period, but relative canopy thickness was not visibly reduced on SB-13 and CF-3 cores. A chiller and submersible pump (AquaEuro Systems), held at a rate of 10-18 L min^{-1}, were used to circulate tap water through the tank with water (T_{water}) set at 18.3 ± 1.3ºC, which was representative of local shallow groundwater in East Wareham, Massachusetts (C. Kennedy, unpublished data). Water temperature in the tank (T_{water}) and air temperature (T_{air}) in the growth chamber were continuously recorded using a HOBO U12 stainless temp logger (T_{water}), and HOBO U23-001 Pro V2 ext. sensor (T_{air}) (Onset Computer Corporation).

Light and humidity parameters were selected that would promote cranberry plant growth. We used in-season mean humidity values of 70% between 5:00 AM and 8:00 PM, and 50% from 8:01 PM to 4:59 AM (Weather History, 2019). Light levels were based on previous growth chamber experiments on cranberries (Kumundini, 2004; Pelletier et al., 2016a), which indicated optimal conditions with light at 40% capacity (out of photosynthetic photon flux density (PPFD) of 1000 μmol m^{-2} s^{-1}) between 5:00 AM and 10:00 AM, 60% capacity between 10:01 AM and 2:00 PM, and back to 40% capacity between 2:01 PM and 8:00 PM. The chamber was dark between 8:01 PM to 4:59 AM. Carbon dioxide levels were set to local ambient conditions (~400 ppm).

In growth chamber experiments, we measured the responses of θ_g, θ_v, ψ, and T_{soil} to varying water table depth and T_{air}. While T_{water} was held constant, we systematically varied lowered the water depth for T_{air} held at 18.3ºC, 23.9ºC, and 29.4ºC, representative of temperatures below, within, and nearing above ideal for maximum cranberry CO_2 acquisition (Pelletier et al., 2016a). Measured T_{air} values were within ±0.6ºC of target temperatures, listed above throughout each experiment (5-10 d). A small circulating fan (Turboforce power, Honeywell) was added to the chamber to facilitate uniform T_{air} within the growth chamber. At each T_{air}, water depth was held constant at 0 (saturated), 10, 20, 30, and 40 cm below the soil surface with a Mariotte bottle for 24 hr, then sequentially lowered using a peristaltic pump (Geopump 2).

We continuously (1-min intervals) monitored θ_v and T_{soil} at the 0-5 cm depth. Data on θ_v (±2%; ECHO EC-5, METERgroup) and T_{soil} (±0.01°C; model '107', Campbell Scientific) were recorded on a CR1000 datalogger (Campbell Scientific). We conducted periodic measurements of ψ at the 0-5 cm depth with a soil tensiometer (TM-31, Soil

Measurement Systems), which consisted of a narrow (2-cm diameter), 30-cm long PVC pipe with a 5-cm long porous ceramic cup. Values of ψ were recorded with a tensiometer (Soil Moisture Systems). We measured $T_{surface}$ with an E5 handheld thermal camera (FLIR), which was set to a focal length of 0 m.

3.3 Field Demonstrations

We recorded ψ in the field at the 0-5 cm depth with soil tensiometers (TM-31, Soil Measurement Systems), as in the lab experiments. Tensiometers were installed in a hole with a soil slurry, using standard methods (Shock and Wang, 2011). Tensiometers require wet conditions for their installation to ensure good soil contact and to prevent damage. We intended to install 12 tensiometers on each section; however, due to restrictions and damage to some tensiometers, this was not possible. We installed 12 tensiometers on SB-13, 12 on CF-3, 10 on CF-2, eight on CF-1, and seven on CF-0 to a depth of 12 cm (Figure 5). We measured ψ on a weekly to bi-weekly basis.

We collected soil samples to determine θ_g at the same location where we conducted field measurements of θ_v and ψ (Figure 5). We collected 2-cm wide, 12-cm long cores with a classic footstep soil probe (Model LS, Oakfield Apparatus). Samples were placed in plastic resealable bags and either processed immediately or refrigerated to prevent evaporation. Samples were homogenized by removing all plant material and debris over 2.5 mm. Soil was placed into tared aluminum boats, weighed, and dried in a 60°C oven for at least 48 hr before being weighed again. Change in water weight was used to calculate the mass of water contained per mass of soil (Bilskie 2001).

We conducted point measurements of θ_v using a TDR 350 fitted with 7-cm rods (FieldScout; Spectrum Technologies), which allowed for rapid, intensive measurements of θ_v. The TDR (time-domain reflectometer) measures soil water content through the generation and reflectance of an electrical pulse between two parallel metal rods. The transmission of this pulse between rods measures the permittivity of the soil (dependent upon θ_v). High TDR permittivity indicates wet soil. The TDR expresses soil moisture as a value of volumetric water content, a ratio of water volume to soil volume. In addition to spot measurements, the TDR 350 was used to map soil moisture with high-density point sampling (~150 points, or 50-100 points ha^{-1}, at CF-3 and SB-13, respectively).

We conducted field demonstrations on sites SB and CF, comparing UAS-collected imagery to conventional measurements of soil moisture and bog temperature. The initial UAS imaging over site SB was conducted on June 26, 2019 and continued at approximately bi-weekly intervals through mid October. For site SB, a comprehensive, season-spanning library of images was obtained. Imagery was first collected from site CF on Aug. 5, 2019. Final images were collected on Oct. 16, 2019. Table 1 displays the locations and dates of field data collection,

We collected UAS images using a Matrice 100 UAS platform (Figure 6). The M100 has a total takeoff capacity of 3600 g and is capable of sustained flight of 11 min with one battery pack. Prior to field season, the M100 was modified to carry an additional battery, which brought the flight time up to approximately 22 min, depending on wind conditions. Seven intelligent flight batteries, LiPo 6S 4500mAh, model TB48D (DJI), were also utilized. This combined battery life allowed for an extended back-to-back

potential flight time of over 77 min. Two cameras were attached to the M100, to collect thermal and NDVI imagery.

Flights were conducted at 60 m at a flying speed of 8 m sec^{-1}. These flight parameters were selected following several test flights during the Summer of 2018, which provided data on the parameters that would provide the best balance between efficient speed of collection and high-quality imagery. A flight over site SB covered 4.7 ha in <9 min. Carverside flights were split into two parts. The first incorporated the 3-yr and 0-yr planting, covering the 6.5-ha area in <10 min. The second flight covered the 1-yr and 2-yr plantings, a 5.5-ha area, in <9 min. Still images were collected along specific GPS tagged transects and then stitched into orthomosaics for all flights. These images were then manipulated in a high quality .tiff format and were analyzed in QGIS.

We used a Zenmuse XT thermal camera (FLIR/DJI) to collect thermal images depicting the surface temperature of sites SB and CF. The Zenmuse XT is a high sensitivity uncooled vox microbolometer thermal camera with a frame rate of 640/30 frames sec^{-1} with a sensitivity of <50 mK at f/1.0. The Zenmuse mounts with a DJI gimbal attached to the forward bottom plate of the M100. This mount was hardwired into the M100 mainframe and power supply, reducing weight but also battery life. The gimbal attachment allowed the Zenmuse to have a 360-degree range of smooth motion via the M100 controller. The camera is capable of collecting either still photos or video. We collected still thermal images at sites SB and CF, on the dates listed in Table 1. Images were initially collected during mid-day to avoid cloud cover. However, to avoid the confounding influence of surface warming sunlight, one flight was conducted at sites SB and CF between 9:00-10:30 PM on Aug. 5, 2019.

We used a Parrot Sequoia multispectral camera to collect images used to calculate NDVI for sites SB and CF. NDVI is calculated using the ratio of reflectance of visible and infrared light (Zhang and Kovaks, 2012; Mallick et al., 2013). These multispectral images were also used to stitch RGB (Red-Green-Blue) or 'normal' coloration images. Multispectral cameras capture image data at defined wavelengths ranges within a spectrum (Oudemans et al., 2002; Mallick et al., 2013). A sunlight sensor was permanently mounted on the top plate of the M100. It continuously adjusted image capture depending on current light conditions. We acquired a 3-D printed gimbal by Copterlab (France), which secured the Parrot Sequoia to the lower battery bay centered underneath the UAS. This gimbal allowed both cameras to be deployed at once, making image collection simultaneous and halving required flight time. The Parrot required an external power source that was provided by a battery pack 6700mAh power bank (Ravpower).

The Parrot has five separate cameras. One is a 16 MP (megapixel) RGB camera with a definition of 4608x3456 px (pixel), which captures RGB images. In addition, there are four 1.2 MP global shutter single-band cameras. These cameras are separated into four separate bands, measured in nanometers (nm). Measured multispectral bands include green (550 nm), red (660 nm), red edge (735 nm), and near-infrared (790 nm). Each of these cameras has a definition of 1280x960 px. Reflectance values from the near-infrared and red wavelengths were used to calculate an NDVI value for each px of stitched orthomosaics (Oudemans et al., 2002; Mallick at al, 2013). Individual images from both thermal and multispectral flights were GPS tagged. These images were delivered to the

company Skycision (Skycision.com), who were contracted to stitch orthomosaics and return high-resolution (.tiff) images.

3.4 Statistics

Least squares linear regressions were fit to datasets ψ, θ_v, and θ_g, T_{water}, T_{soil}, $T_{surface}$, T_{air}, and water table depth collected in the growth chamber. A linear relationship between θ and ψ has been established in literature (Jeranyama et al., 2017), as has a linear relationship between θ and ψ and water table depth (Pelletier et al., 2015b). Least squares linear regressions were analyzed using a REG procedure in SAS (SAS Institute Inc.; Cary, USA). The confidence limit engaged to determine if the R-squared was significant was $P<0.5$. For point measurements and θ_v mapping, analysis of spatial patterns in θ_v was carried out in ArcGIS 9.1 (ESRI; Redlands, CA). Spatial interpolation was conducted using ordinary Kriging. The identification of non-random (clustered) spatial patterns in θ_v was accomplished using Moran's I (Spatial Statistics Toolbox, ArcGIS 9.1) to quantify spatial autocorrelation.

CHAPTER 4

RESULTS AND DISCUSSION

4.1 Growth Chamber Experiments

Least squares linear regression analysis was used to evaluate relationships between water table depth, volumetric water content (θ_v), and soil tension (ψ) for soil cores collected from SB-13, CF-0, and CF-3. Results showed that θ_v and ψ were tightly associated with water table depth (Figure 7), as would be expected for sandy soil (Lampinen, 2000). In general, ψ was a better predictor of water table depth than θ_v, which we attributed to uncertainty at the lower end of the measurement range of θ_v (± 0.02). Using our experimental data, we developed a combined predictive equation of ψ for cranberry farms in Massachusetts:

$$\psi = 0.0943x + 0.136 \; R^2 = 0.994, \qquad (2)$$

where ψ has units of kPa (5-cm depth) and x is water table depth relative to the soil surface in cm. Based on these results and the irrigation thresholds reported in Jeranyama et al. (2017), we recommend that growers maintain a water table depth of 20 to 50 cm below the soil surface, equating to -2.0 to -5.0 kPa. To maintain this water table depth, open ditches should be dredged to at least 50 cm. To anchor runners and promote upright growth, growers periodically apply thin layers of sand either on ice, in water or directly on the vines (Sandler and DeMoranville, 2008). All efforts should be made to apply sand

uniformly (Hunsberger et al., 2006), as sand thickness affects water table depth (x) and thus ψ (Eqn. 2).

Least squares linear regression analysis was used to evaluate relationships between soil moisture (θ_v, ψ) and soil temperature (T_{soil}) and near-surface temperature ($T_{surface}$). Experiments were conducted using a constant water temperature (T_{water} = 18.3°C) and measuring T_{soil} and $T_{surface}$ in response to air temperature (T_{air}) adjusted to 18.3°C, 23.9°C, and 29.4°C. Continuous (15-min intervals) monitoring of T_{water} indicated that experiments were conducted reasonably close to our "target" T_{water} of 18.3°C with values ranging from 17.9°C to 18.5°C with one exception, 20.5°C, which was measured in response to the highest T_{air} (29.5°C) for SB-13 (Table 2). We expected that T_{air} would influence T_{water} but cannot explain why this effect was pronounced in SB-13 compared with CF-0 and CF-3. However, we can report that this effect was not due to differences in our "target" T_{air}, which was within <0.71°C of the targeted setpoint (Table 2).

We observed a significant correlation (R^2 >0.75, P-value <0.05) between differences in T_{air} and T_{water} ($\Delta T_{air\text{-}water}$) and water table depth for T_{air} of 18.3°C ('107' sensor only), 23.9°C, and 29.4°C (Table 3). However, regression slopes were only significant for the two highest values of $T_{air,}$ illustrating that soil moisture inferred from T_{soil} is dependent on $\Delta T_{air\text{-}water}$. For example, at T_{air} = 18.3°C, T_{soil} varied by <2°C for water-table depths ranging from 0 to 50 cm. In contrast, T_{soil} ranged from 4-6°C at T_{air} = 23.9°C and from 6-10°C at T_{air} = 29.4°C for water table depths of 0 to 50 cm. We observed linear relationships between T_{soil} and θ_v and ψ that were similar to those for T_{soil} and water table depth (data not shown).

Theoretically, at full saturation (water table = 0 cm), differences between T_{soil} and T_{water} would be zero, with T_{soil} approximating T_{water} (18.3°C). Conversely, after complete drainage, T_{soil} would equal T_{air}. However, we found that T_{soil} did not follow these theoretical trends for SB-13 and CF-3, although the trend was observed for $T_{surface}$ in CF-0 (non-vegetated). Soil texture and organic matter content may have had an impact on the observed results, with the sifted, low organic matter containing unplanted cores (CF-0) most accurately following the theoretical trend. The amount of soil organic matter has been demonstrated to impact soil water-holding capacity (Saxton and Rawls, 2006). At levels below 8%, increasing soil organic matter has been observed to increase water-holding capacity, or the ability for soil to physically hold onto water via cohesion (Saxton and Rawls, 2006). This trend may explain the higher θ_v observed in SB-13, and to a lesser extent, CF-3 cores (Figure 8). This behavior of water holding may have prevented soil temperature from reaching air temperature despite lowering of the water table.

Near-surface temperature ($T_{surface}$) was also correlated with water table depth (R^2 >0.5), but linear regressions were less significant than those based on T_{soil}, perhaps due to the confounding influence of plant material (Saxton and Rawls, 2006). Even so, accurate predictions of water table depth were achieved with $T_{surface}$, as were predictions of θ_v and ψ. These proof-of-concept results were motivation to explore the use of $T_{surface}$ in mapping soil moisture variation in peatland and upland farms. We acknowledge limitations of the method concerning $\Delta T_{air\text{-}water}$ but believe that the potential time savings warrants further investigation.

4.2 Field Demonstrations

4.2.1 Point measurements of ψ, θv, and θg

During the 2019 growing season (June to Sep.), field data of ψ, θ_v, and θ_g were collected from 8-12 monitoring locations on SB-13, CF-1, CF-2, and CF-3 (Figure 9). During the study, mean values of θ_v were 34.4% for SB-13 and 7.9%, 4.2%, and 2.2% for CF-3, CF-2, and CF-1, respectively. Coefficients of variation about mean θ_v (i.e., the average of the standard deviation divided by the mean for different sampling runs) was 9.0% for SB-13 and 4.5% CF-3. These patterns were consistent for ψ and θ_g. A comparison between SB-13 and site CF farm units showed that upland cranberry farms were generally four times drier and two times more homogenous than peatland farms. Site CF soils were, as a trend, observed to be below field capacity, whereas SB-13 remained well above the threshold.

Significant spatial and temporal variability of soil moisture was observed in SB-13 (Figure 9, peatland farm panel). On SB-13, point measurements of θ_v and θ_g varied spatially by 10% to 15% (note differences are absolute rather than percent). Values of ψ ranged from 0 to -5.0, with a mean of -2.4 kPa, falling within recommendations by Jeranyama et al. (2017). Temporal variation in θ_v was extensive due to seasonal irrigation and rainfall inputs as well as inadequate drainage, with mean values ranging from 14.6% to 48.2% over a 2-wk period in July. A general pattern of decreasing (drying) values of ψ, θ_v, and θ_g was punctuated by wetting periods due to irrigation or rainfall events.

ψ on CF-3 remained within the recommended range of -2.0 to -5.0 kPa, with an average of -3.3 kPa. This ψ was drier than the mean ψ of -2.4 kPa observed on SB-13, but still within the recommended range for Massachusetts (Jeranyama et al., 2017). Site CF, in general, was drier than site SB. However, this site also fell within the drier range of recommendations for Massachusetts cranberry farms. In comparison, ψ suggestions for other cranberry regions range between -4.0 and -7.0 kPa (Pelletier et al. 2015a, b; Caron et al. 2017). These recommendations are made for cranberry farms located in Quebec, which are engineered on top of parent soils with very different hydrogeological characteristics than those found in Massachusetts. Water tables are deep on Quebec cranberry farms, and soils are extremely well-drained. While ψ is independent of soil type (Figure 7), the relationship between θ and water table depth does vary based on soil texture (Figure 8). The current ψ, θ_v, and θ_g recommendations for Massachusetts cranberry farms works best for peatland farms with limited drainage capacity. Cranberry is a wetland, C3 plant with a shallow root system. Its near-surface ψ needs are wetter than other crops due to these characteristics. The shallow root system of cranberry necessitates a near-surface water table to allow plants to maintain ideal hydration. Conversely, these shallow roots also assist cranberry in avoiding hypoxia during periods of elevated soil moisture.

In comparison to cranberry, deeply rooted non-wetland C3 plants, including cole crops and sweet potato, have only slightly drier ψ guidelines, in that that soil tension measured from the soil surface (10-30 cm) must be interpreted depending upon the depth of the plant root zone. Cole crops, with a root depth of up to 90 to 120 cm grow best within a range of -6 to -12 kPa (when ψ is measured in the top 30 cm) (Shock and Wang,

2011). For sweet potato, water needs change depending on life stage and the extent of root growth, with early (immature crop) irrigations thresholds at -2.5 kPa, and later (established crops) at -10.0 kPa (when ψ is at 23 cm) (Smittle et al., 1990). Sweet potato roots grow to depths beyond 40 cm, necessitating drier soil conditions and a lower water table than is recommended for shallow rooting plants such as cranberry (Shock and Wang, 2011). Cranberry growers are increasingly planting large-fruited, vigorous hybrid cultivars. These plants may have structural or physiological differences that impact water requirements. It is important for individual growers to assess the water needs of their crop and set target ψ ranges that are individualized based upon parent soil material, available water table depth, and cultivar.

Despite spatial and temporal variability, patterns of temporal variation in soil moisture were similar among individual points in SB-13 (Figure 9), indicating persistent dry soil zones throughout the growing season. In particular, two locations on the north end of SB-13 (points 11 and 12) were consistently 1.3 to 1.7 times drier than the other sampling points. These point measurements coincided with a section of the farm that was extended during the 2006 renovation. As a result, the north end of SB-13 does not include a water-confining peat layer, which likely contributed to the relatively dry soil observed at points 11 and 12.

Soil moisture variation on site CF farm units (CF-0, CF-1, CF-2, CF-3) was relatively low compared with SB-13, averaging -3.3 kPa for ψ, and ranging between 4% to 12% for θ_g, and 3% to 15% for θ_v. We attribute this minor soil moisture variation to uniform sand thickness and texture, as well as uniform irrigation through subsurface tiles. Although sub-irrigation was not the principal irrigation method, it was used to maintain

water table depths throughout the growing season. We concluded that the use of subirrigation via adding water to irrigation canals most likely resulted in anomalous point measurements on Sep. 17, 2019. Water filled ditches to capacity; it was noted that water was encroaching onto the farm surface at this time. On this date, the two sampling points closest to the irrigation canal exhibited θ_v values of 22%; this level of θ was twice as high as the θ for the rest of the farm (Figure 9).

4.2.2 High-Density Mapping of θ_v

SB-13 exhibited significant spatial variation in θ_v, with values ranging from 0-36% θ_v and averaging ~25%, remaining well above the field capacity of ~5-15% θ_v for these soils (P. Jeranyama, pers. comm., 2020) (Figure 10). Dry areas of the farm were located along edges, particularly over renovated sections of the farm that lacked underlying peat. The central ditch (Figure 5) was most likely responsible for locally high θ_v along the center of the farm, especially since ditches were often used to subirrigate the farm. The observed patterns in spatial variation of θ_v was representative of maps of θ_v collected earlier in the 2019 growing season, as well as during 2018 and 2017 (data not shown). The results indicated that SB-13 has consistent 'dry spots' that require targeted management approaches.

Spatial variation of θ_v in CF-3 was two times lower than SB-13, with values ranging from 2-8% and averaging 5% (Figure 10). When the relative size of SB-13 and CF-3 was taken into account, the lack of variation in CF-3 was even more noticeable, with the length of CF-3 equal to 2.5 times the length of SB-13. On site CF, areas of the

farm nearest to irrigation canals were wetter than other areas of the farm, despite encroachment not being notable during point collection. This observation was attributed to water being fully raised within the canal at the time, as well as the uniform, low topography of the farm, which allowed for water encroachment. Additionally, site CF does not employ the interior ditches used on site SB (see Figure 5). Interior ditches were associated with trends of increasing soil moisture towards the center of SB-13 and increased overall variability of soil moisture on the farm. The absence of interior ditches on site CF may have contributed to relatively uniform values of θ_v.

Geospatial modeling of θ_v confirmed that SB-13 was wetter and exhibited greater soil moisture variation than CF-3. Uniform soil moisture is easier to monitor and manage, and cranberry farmers may save both time and money when a single, well-placed point measurement can provide representative information of the farm. Additionally, avoidance of hypoxia is indispensable for attaining high levels of cranberry yield (Caron et al., 2017; Kennedy et al., 2017; Jeranyama et al., 2017). Pelletier et al. (2015b) recommended initiating irrigation when ψ dropped below -7.0 kPa and suggested that dry conditions (an average water table depth of 60 cm), in general, resulted in maximum yields. While these recommendations were made for cranberry farms, hydrogeology and parent soil characteristics in Québec and Massachusetts are vastly different. Soils at the sites assessed by Pelletier and Caron were located above well-draining mineral soil. These farms, in general, have high drainage capacities and low topographical and hydrological irregularities (Caron et al., 2017).

Observations of θ_v and ψ on site CF show adherence to recommendations similar to those for Québec cranberry farms. Site CF, constructed over mineral parent soils,

allows for adequate and uniform drainage. These characteristics simplify the management of site CF and allow for the maintenance of dry soil conditions. Site SB, due to its shallow water table, requires more intensive management, including the decision of where to place a soil moisture sensor. A soil moisture sensor installed in the wrong area may result in an inappropriate irrigation regime for the majority of the farm. Additionally, the presence of wet and dry spots makes it impossible for the entire farm to be within an ideal θ range simultaneously. This has the potential to curtail vine establishment, support disease populations, depress plant respiration, and cumulatively reduce yield quality and quantity.

4.2.3 Unmanned aerial systems (UAS)

UAS images were initially collected in the late morning or early afternoon, but these images exhibited irregularities (Figures 11, 12, and 13), potentially due to the effects of direct sunlight on the plant canopy. As such, we conducted a night-time (9:30 PM-11:00 PM) UAS flight on Aug. 5, 2019, at both SB-13 and CF-3, which improved the display of moisture-temperature relationships compared to IR imaging during the day (Figure 11). For SB-13, the values of $T_{surface}$ ranged from 19°C to 24°C. Spatial variation in $T_{surface}$ exhibited a pattern that was similar to that observed for θ_v (Figures 9, 10), with cool temperatures clustered towards the center of the farm, and prominent warm spots along the farm edges, particularly in the northern area where peat was absent.

The night-time UAS flight over CF-3 recorded that the $T_{surface}$ was relatively warm and uniform compared with SB-13. For the majority of CF-3, $T_{surface}$ ranged between 23°C and 24°C. A notable exception was a section in the northeastern corner of

the farm, which was adjacent to an irrigation canal (Figure 11). We surmised that the cool values of $T_{surface}$ for this section of the farm were due to the encroachment of cold irrigation water onto the farm. Full ditches had previously been observed to impact soil moisture in this section of the farm, as evidenced by measurements of θ_v on Sep. 17, 2019 (Figure 9). However, this pattern was not observed in our geospatial model of θ_v (Figure 10), which was based on point measurements of θ_v that were collected when the surface water in the irrigation canal was low.

UAS thermal imaging also illustrated the effects that canal seepage had on $T_{surface}$ in CF-2 and CF-1 (Figure 11). In particular, CF-2 was cool in areas adjacent to an irrigation canal while remaining warm in sections of the farms located >20 m from the irrigation canal. Values of $T_{surface}$ ranged from 19°C to 23°C in CF-2. By comparison, CF-1, which was apparently not influenced by canal seepage, had values of $T_{surface}$ that ranged from 23°C to 24°C. The tighter temperature range observed on CF-3 supports predictions of lower amounts of variation in temperature when compared to SB-13.

Despite reduced contrast, daytime IR images were able to identify potential irrigation problems, as observed in Figure 12, which illustrated localized hot spots that were consistent with irregularities in sprinkler irrigation. The shape of the IR temperature anomalies included a localized cold center surrounded by a circular hot area, which we interpreted to be caused by a malfunction in an irrigation sprinkler head. Warm anomalies ranged from 3°C -4°C above the average temperature of the farm (~33°C). Our empirical relationship between θ_v and $T_{surface}$ suggests that these hot spots are due to relatively low θ_v; that is, these hot spots were likely not being irrigated. The identification of irrigation issues by thermal IR imaging via UAS presents several advantages. In this study, we

evaluated a 14-ha farm unit in approximately 40 min, without walking or driving onto the farm and damaging fruit. Generally, the use of diagnostic UAS technology could save time and money for operators of cranberry farms (Oudemans et al., 2002; Mallick et al., 2013; Mulla, 2013; Bellvert et al., 2014; Chang and Hsu, 2018)

UAS images of NDVI and RGB were used to assess plant health for upland and peatland farms. Figure 14 displays the calculated NDVI of the entire areas of CF-3 and site SB for Sep. 17, 2019. Site SB, which consists of established 13-yr-old vines, exhibited higher NDVI, with values ranging from 0.8 to 1. Within site SB, NDVI was predictably lower along the edges of individual sections, as well as in areas that experience high foot-traffic or are used for destructive experimentation. NDVI of CF-3, by comparison, ranged from 0.6 and 0.8. We attribute differences in NDVI between site SB and CF-3 to the respective ages of the vines, although cultivar and fertilizer management may have also affected NDVI (Sandler, 2009).

RGB, or visual color, images of site SB were collected at three different times during the growing season (Figure 15). The first image (Figure 15A), collected on July 3, 2019, shows the bog during bloom, which gives the image a white cast due to the high numbers of pale cranberry blossoms. The second image (Figure 15B) was taken on Aug. 1, 2019, when berries are formed but only beginning to turn red. The third image (Figure 15C) was collected on Sep. 19, 2019, less than 1 mo from harvest. At this date, the majority of berries were full sized and red, coloration that was apparent in the image. These results suggest that remote sensing techniques may be a valuable tool for assessing plant health and development in cranberry farms (Oudemans et al., 2002; Zhang and Kovaks, 2012; Zhang and Zhou, 2016). For instance, applications of fertilizers and

pesticides are often scheduled based on bloom or the stage of fruit development. These assessments are typically made following field observations (collected on foot), which can be time-consuming and lack accuracy for large farms. The ability to quantify percentages of bloom or fruit development appears to be a useful application of UAS technology on cranberry farms.

4.3 Limitations of UAS use in Cranberry

While some limitations have been reported in other crops (Mulla, 2013; Bellvert et al., 2014; Chang and Hsu, 2018), several important limitations exist for the use of UAS remote sensing on cranberry farms. A major limitation for the use of UAS imaging of cranberry relates to the growth patterns and vining characteristics of the cultivated plant. Farmed cranberry forms a continuous mat of vegetation, which makes it extremely difficult to identify individual plants within a farm (Eck, 1990). Similar limitations are experienced by those using UAS systems on turf, another crop which forms a continuous mat (Zhang et al., 2019). Typically, plants imaged with UAS technology may be individually identified, and bare soil may serve as a reference surface (Jones, 2004; Bellvert et al., 2014; Zhang and Zhou, 2016). For row crops, including grapes, researchers or farmers may interpret NDVI or thermal imagery to identify an individual plant that is experiencing stress (Bellvert et al., 2014; Zhang and Zhou, 2016; Chang and Hsu, 2018). In cranberry, it is challenging to pinpoint an individual cranberry plant, or to apply certain indices that require a reference surface (Zhang and Zhou, 2016).

The presence of a thick, continuous plant canopy also poses issues for assessing direct soil surface temperature. As observed in growth chamber experiments, thermal

cameras more accurately determined surface temperature on cores with minimal vegetation (Figure 8). The plant canopy blocked thermal cameras from directly measuring the soil surface. This issue may be exaggerated during periods of bright sun. During sunlight, all vines were warmed as the ambient temperature changed. Additionally, plants responded to sunlight and increasing temperatures by respiring for cooling and for energy fixation (Bland et al., 1995; Hattendorf, 1996; Jones, 2004; Blatt et al., 2014). These factors made it difficult to confidently relate plant canopy temperature to soil water variability. Thermal images collected during the day displayed little variation, suggesting that these images are not ideal for the differentiation of temperature and moisture variability (Figures 12, 13). In response to issues with day-collected image quality, we conducted thermal flights after sunset (Figure 11). This choice increased our confidence that the temperature variations observed were not influenced by warming sunlight or plant physiological responses, and better represented soil moisture differences.

Additionally, we encountered a common limitation in the use of UAS for precision agriculture: a lack of image detail (Ishimwe et al., 2014). Our research collected images from a flight height of 60 m, while flying at 12 m sec^{-1} in order to record in a timely manner. This provided a relatively low-resolution image, with one px equaling ~5 cm^2 for the multispectral camera, and ~10 cm^2 for the thermal camera. Future flights conducted at a lower height would increase image resolution and more accurately assist in the identification of stress or varietal differences in cranberry (Bellvert et al., 2014; Ishimwe et al., 2014).

The impact of canopy density on the interpretation of both NDVI and IR thermal images merits further advancement and testing before the technology may become practical for adoption by cranberry farmers. Lower altitude or slower image collection flights may be used to collect more detailed images of cranberry farms. Additionally, findings suggest that UAS tools may be best employed at early stages of the renovation process, to inform farmers of irregularities (e.g., irrigation issues or areas of water encroachment when water level is high in irrigation canals) before vines are planted, or while vines are in their first years of establishment (Sandler, 2009).

CHAPTER 5

CONCLUSIONS

The Massachusetts cranberry industry is undergoing changes to remain competitive in a global market. The understanding of soil water patterns, processes, and predictability has the potential to improve water management and increase yield on Massachusetts cranberry farms.

This research compared the processes affecting soil moisture on peatland and upland cranberry farms. Soil temperature and near-surface IR temperature were correlated with soil moisture variation, but temperature-moisture relationships were strongest for soils with lower vegetation coverage and organic matter content. In the field, $T_{surface}$ and θ_v followed similar patterns, suggesting that near-surface IR temperature measured with a UAS could be used to rapidly determine large-scale variation in θ_v. Areas of apparent sprinkler malfunction were identified using $T_{surface}$.

Peatland and upland Massachusetts cranberry farms were observed to differ in their soil moisture patterns and trends. Values of θ_v in upland farms ranged from 5-15% throughout the growing season, with minimal variation detected. The exception to this observation was associated with seepage from an irrigation canal adjacent to the farm. In contrast to findings on upland farms, peatland farms were wetter and exhibited higher soil moisture variation, with values of θ_v ranging between 10-40%. Soil moisture in upland farms was two times drier and four times more uniform than peatland farms.

UAS technology requires refinement but shows promise as a tool to aid soil moisture management, canopy assessment, and life stage determination in commercial cranberry production. Thermal images, while sensitive to daytime sun and heat, as well as

lack of reference surface, were able to predict large scale soil moisture trends. Multispectral cameras assessed canopy thickness and plant development. Information captured by multispectral cameras may inform on plant health as well as the level of plant development, or vine establishment. This information is an example of valuable information collected with a UAS that may be used to inform management decisions.

Specific management recommendations for the enhancement of soil moisture conditions on peatland and upland cranberry farms in Massachusetts include support for maintaining ψ, θ_v, and θ_g, within recommended ranges. Correlation between water table depth and ψ suggests that open ditches should be dredged to at least 50 cm to obtain irrigation set points of -2.0 and -5.0 kPa. Individual farmers should carefully assess water needs based upon parent soil material, water table depth, and cultivar selection. Soil texture and water table depth influence the response of θ, and broad recommendations of θ should be individualized in the manner that supports optimal plant health and fruit yield.

Table 1: Schedule of field measurements carried out on cranberry farms over the 2019 growing season in areas of site SB (East Wareham, MA) and site CF (Carver, MA). Field data include point measurements of gravimetric water content (θ_g), volumetric water content (θ_v), soil tension (ψ), and the collection of images using an unmanned aircraft system (UAS), both thermal, recording the infrared temperature of the farm surface ($T_{surface}$) and multispectral (M-Spec). * Indicates UAS night flight, where thermal images were collected.

	θ_g, θ_v, ψ,	θ_v Map	UAS $T_{surface}$	UAS M-Spec	θ_g, θ_v, ψ,	θ_g, θ_v, ψ,	θ_v Map	UAS $T_{surface}$	UAS $T_{surface}$	UAS M-Spec
Location	SB 13	SB 13	SB	SB	CF 0, 3	CF 1, 2	CF-3	CF 0, 3	CF 1, 2	CF 0, 3
6/13/19	X									
6/19/19	X		X							
6/26/19	X	X								
7/3/19	X	X	X	X						
7/16/19	X	X	X							
7/24/19	X									
8/1/19			X							
8/5/19			X*					X*	X*	
8/6/19					X	X				
8/22/19	X				X					
9/17/19	X		X	X	X	X		X		X
10/1/19		X			X		X			

Table 2: Measured air temperature (T_{air}) and water temperature (T_{water}) inside the growth chamber, with +/- standard deviation for soil cores. Cores were collected from cranberry farms over the 2019 growing season from areas of site SB (East Wareham, MA), and site CF (Carver, MA). Cores were labeled by location (sites CF or SB), and by the age of vines growing on top of the soil cores (0 yr, 3 yr, or 13 yr).

Target T_{air} (T_{water})	*Measured T_{air} (T_{water}) °C*		
	CF-0	CF-3	SB-13
18.3 *(18.3)*	18.71+/- 0.02 (18.37 +/- 0.13)	N/A (18.27 +/- 0.16)	18.53 +/- 0.04 (17.93 +/- 0.25)
23.9 *(18.3)*	23.38+/- 0.11 (18.46 +/- 0.17)	N/A (17.08 +/- 0.3)	23.51 +/- 0.02 (18.54 +/- 0.13)
29.4 *(18.3)*	28.82 +/- .71 (18.72 +/-0.12)	N/A (17.81 +/- 0.6	28.84 +/- 0.16 (20.5 +/- 0.47)

Table 3: Least-squares linear regression equations, including P-values and R-squared values for the measured difference between T_{soil}, T_{air}, and T_{water} in growth chamber experiments. P-values of $P<0.05$ were considered significant. IR recorded $T_{surface}$ using an infrared camera (E5, FLIR). '107' sensor (Campbell Scientific) recorded T_{soil} in the top 5 cm of each of three replicate soil cores. Cores were collected from cranberry farms over the 2019 growing season from areas of site SB (East Wareham, MA), and site CF (Carver, MA). Cores are labeled by location (sites CF or SB), and by the age of vines growing on top of the soil cores (0 yr, 3 yr, or 13 yr).

		Infrared Camera			*'107' Sensor*		
		Linear Regression	P-value	R-squared	Linear Regression	P-value	R-squared
CS0	18.3	y = -0.0408x - 2.0179	0.056	0.553	y = -0.0127x - 0.6508	0.043	0.594
	23.9	y = -0.1002x + 0.4037	0.029	0.646	y = -0.0529x + 1.9106	0.001	0.913
	29.4	y = -0.2374x - 0.5072	0.000	0.936	y = -0.1324x + 3.166	0.000	0.979
CS3	18.3	y = -0.1127x - 1.6839	0.085	0.837	y = -0.0304x - 0.3709	0.037	0.927
	23.9	y = -0.1438x + 3.8584	0.037	0.927	y = -0.2137x + 0.8888	0.037	0.927
	29.4	y = -0.1808x + 5.1733	0.096	0.817	y = -0.3251x + 2.542	0.005	0.991
SB12	18.3	y = -0.1086x - 1.1073	0.028	0.654	y = -0.0336x + 0.6254	0.031	0.641
	23.9	y = -0.1212x + 2.5348	0.034	0.627	y = -0.1727x + 0.4683	0.001	0.912
	29.4	y = -0.1287x + 3.7329	0.027	0.658	y = -0.2019x + 1.1748	0.008	0.787

Upland Cranberry Farm, located in Wisconsin

Peatland Cranberry Farm, located in Massachusetts

Figure 1: Images compare peatland and upland cranberry farms. The upland cranberry farm, located in Wisconsin, consists of large rectangular sections. The peatland farm, located in Massachusetts, is irregularly shaped and made up of several smaller sections bisected by drainage canals.

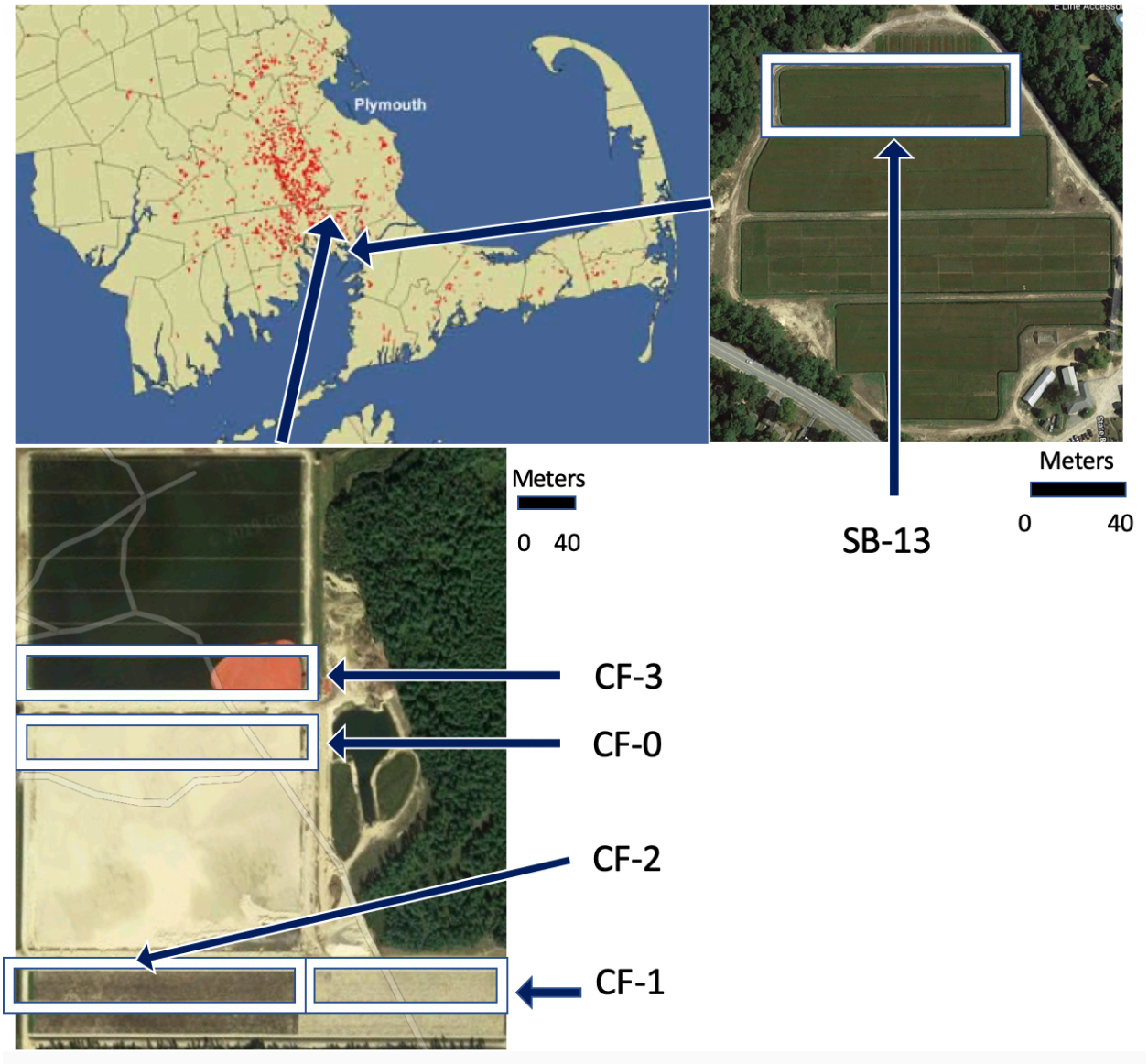

Figure 2: Location of site SB (East Wareham, MA), peatland farm, and site CF (Carver, MA), upland farm. Sections are labeled by the age of vines and located within a map of Plymouth County, with cranberry farms indicated in red.

Vines, CF-1

Vines, CF-2

Vines, CF-3

Vines, SB-13

Figure 3: Photographs of cranberry canopy at site SB (East Wareham, MA), peatland farm, and CF (Carver, MA), upland farm. Photos demonstrate the typical vegetation thickness and are labeled by location (CF or SB), and by the age of vines growing on top of the soil cores (1 yr, 2 yr, 3 yr, or 13 yr).

Figure 4. Photographs from the core extraction and installation process. Cores were extracted from cranberry farm surface at site SB (East Wareham, MA), peatland farm, and site CF (Carver, MA), upland farm. Labeling indicates location (CF or SB), and the age of vines. A. Example of post-core extraction from CF-3, showing homogenous sand with low organic matter. B. Cores extracted from SB-13, showing alternating bands of high organic matter and sand. C. Cores in tank within the growth chamber with water table raised to saturation (0 cm). Tensiometers, EC-5, and '107' sensors were installed into cores.

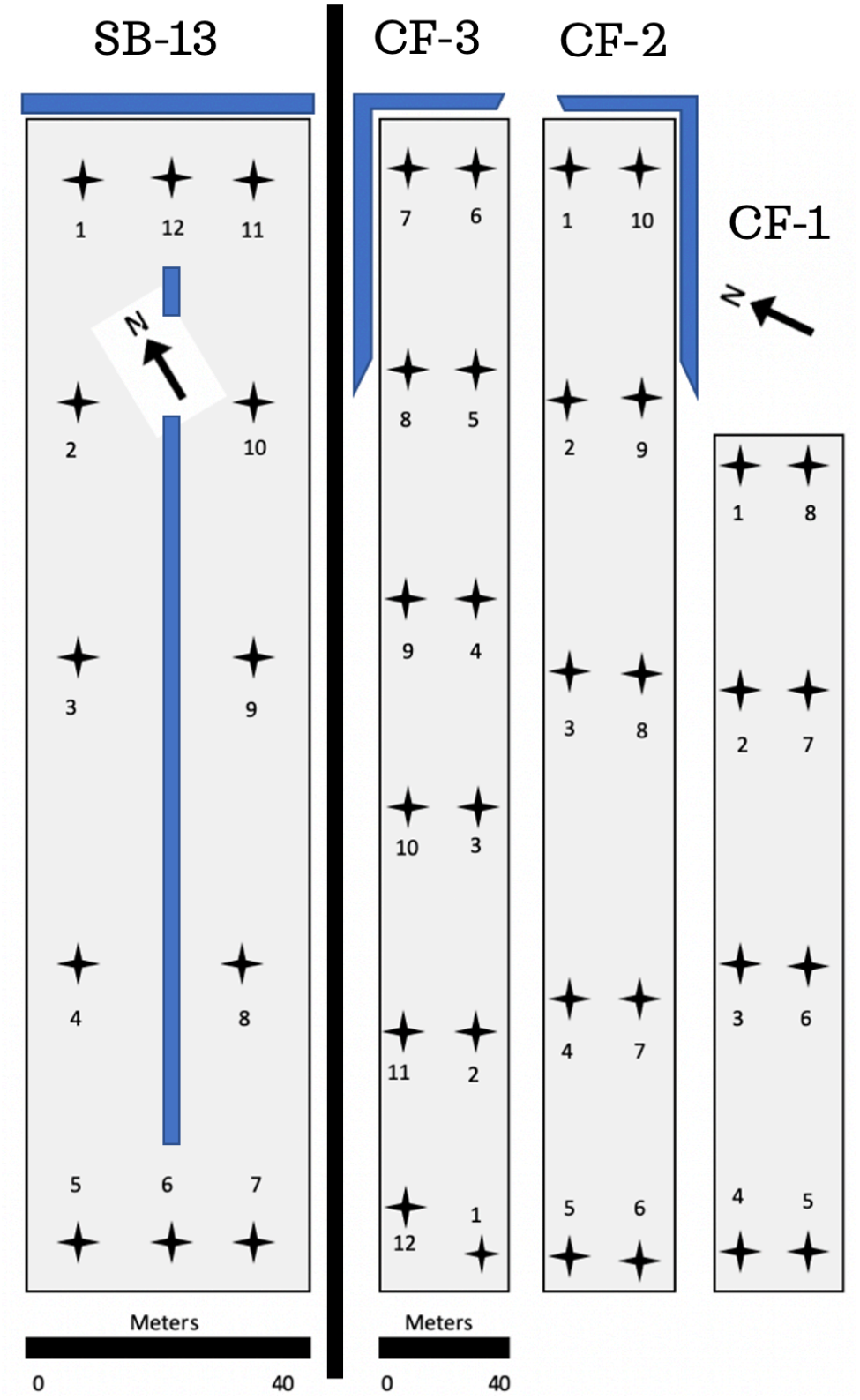

Figure 5: Diagram of the arrangement of point measurements, where tension (ψ), volumetric water content (θ_v), and gravimetric water content (θ_g) were measured. Point measurements were collected from site SB (East Wareham, MA), peatland farm, and site CF (Carver, MA), upland farm. Labeling indicates location (CF or SB), and the age of vines. Left map is SB-13, to the right are CF-3, CF-2, CF-1, and CF-0 as labeled. Blue borders represent the location of irrigation canals.

Figure 6: Image of the Unmanned Aircraft System (UAS) used for image collection. The UAS consisted of a Matrice 100 drone (DJI), mounted with a Zenmuse XT (FLIR) thermal infrared camera, and a Parrot Sequoia multispectral camera (Micasense).

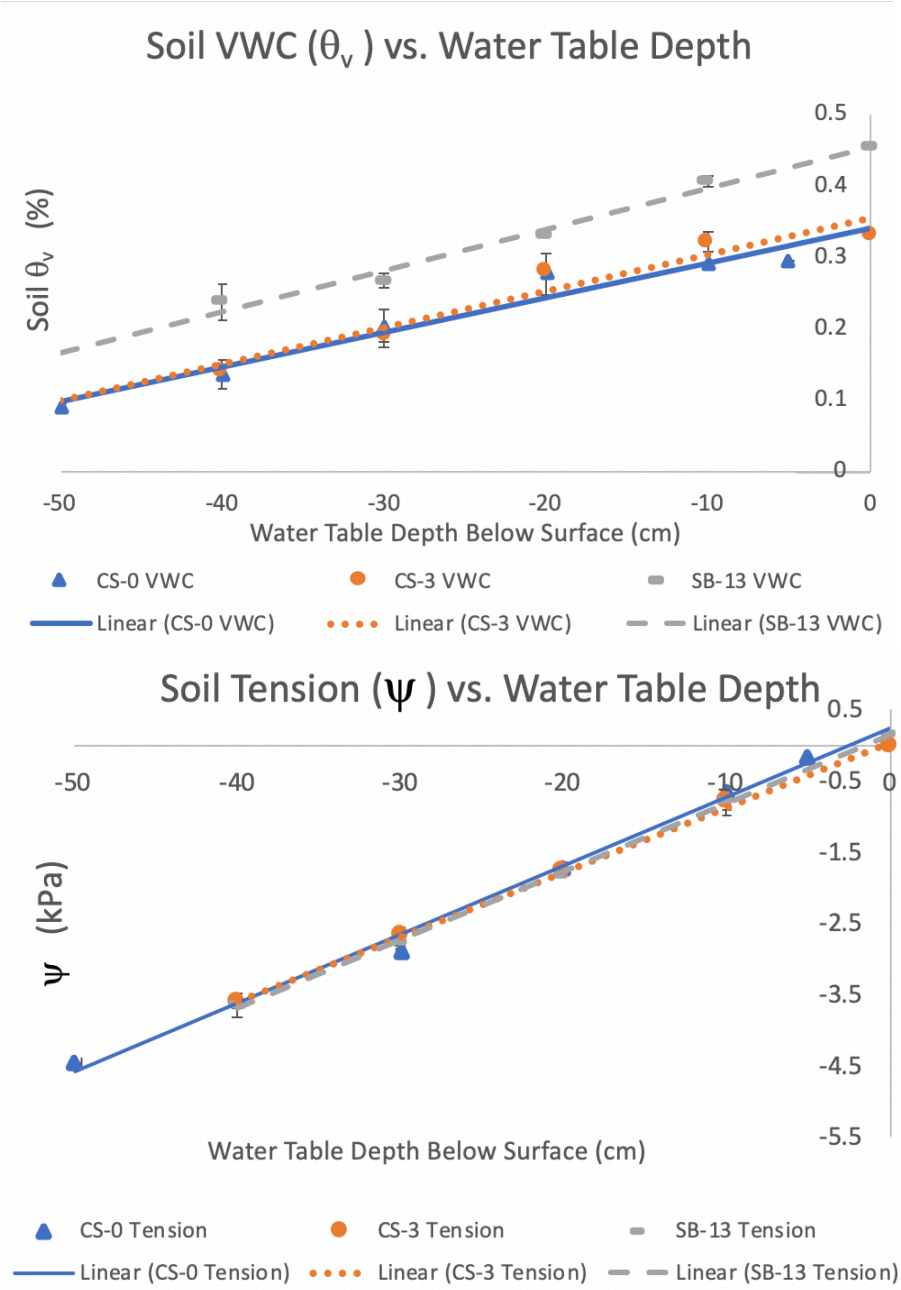

Figure 7: Mean tension (ψ) and volumetric water content (θ_v) from all temperature runs vs. water table depth from cores collected from CF-0, CF-3, and SB-13. Cores were collected from site SB (East Wareham, MA), peatland farm, and site CF (Carver, MA), upland farm, labeled by the age of vines. Temperature runs were pooled to include all temperatures and all locations, N=3 for each location. Trend lines represent linear regressions, and error bars one standard deviation.

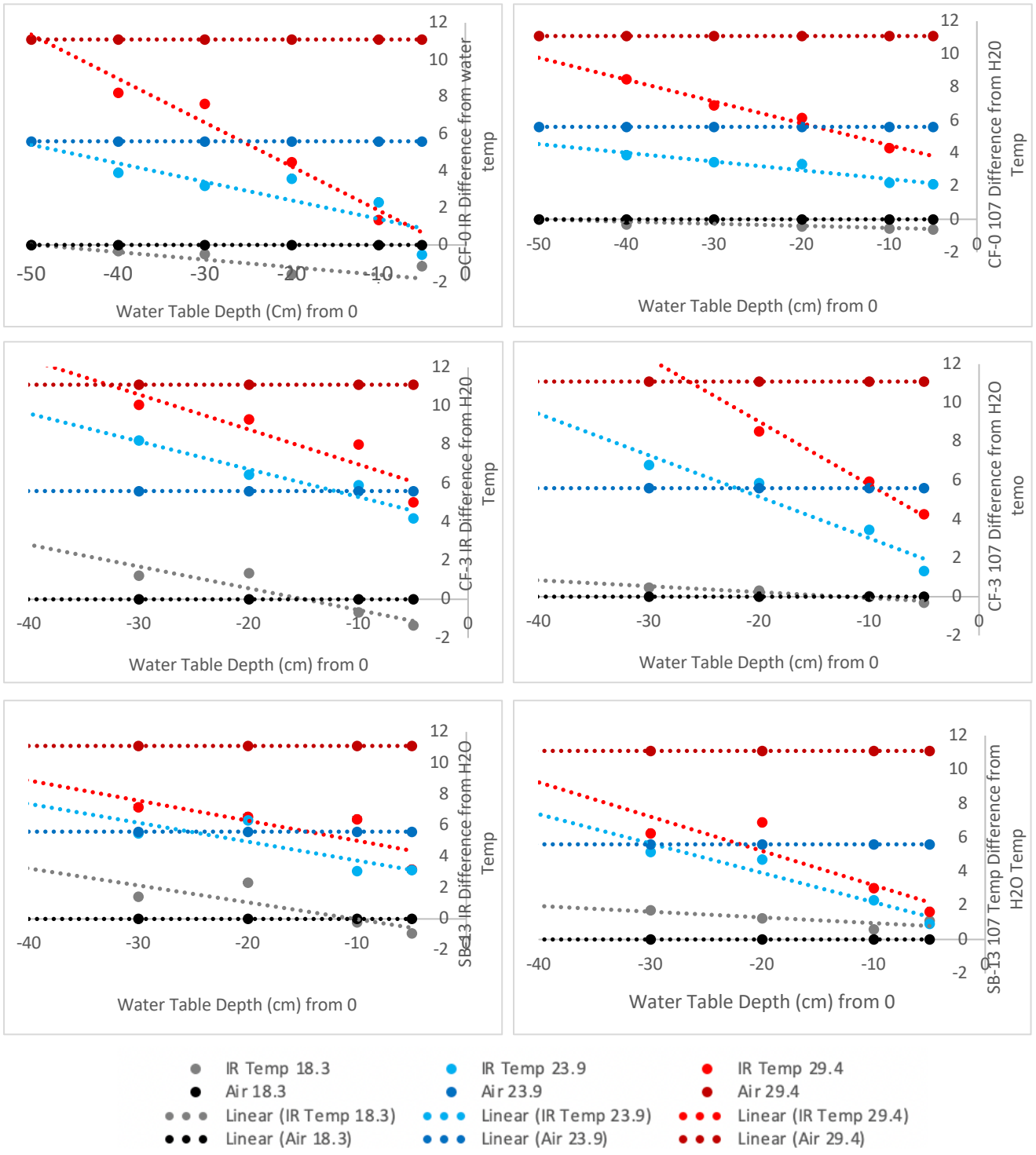

Figure 8: Mean difference between T_{soil} /$T_{surface}$, T_{air}, and T_{water}. $T_{surface}$ was measured with an IR camera (E5, FLIR) positioned directly above the core surface. T_{soil} was recorded using '107' temperature probes (Campbell Scientific), inserted into the top 5 cm of soil. Temperatures were measured as water table depth was lowered by 10-cm increments from a saturated level (0 cm) until the water was removed entirely. Cores containing CF-0 sand were 50-cm tall, while SB-13 and CF-3 cores were 40-cm tall. Cores were collected from site SB (East Wareham, MA), peatland farm, and site CF (Carver, MA), upland farm, labeled by the age of vines.

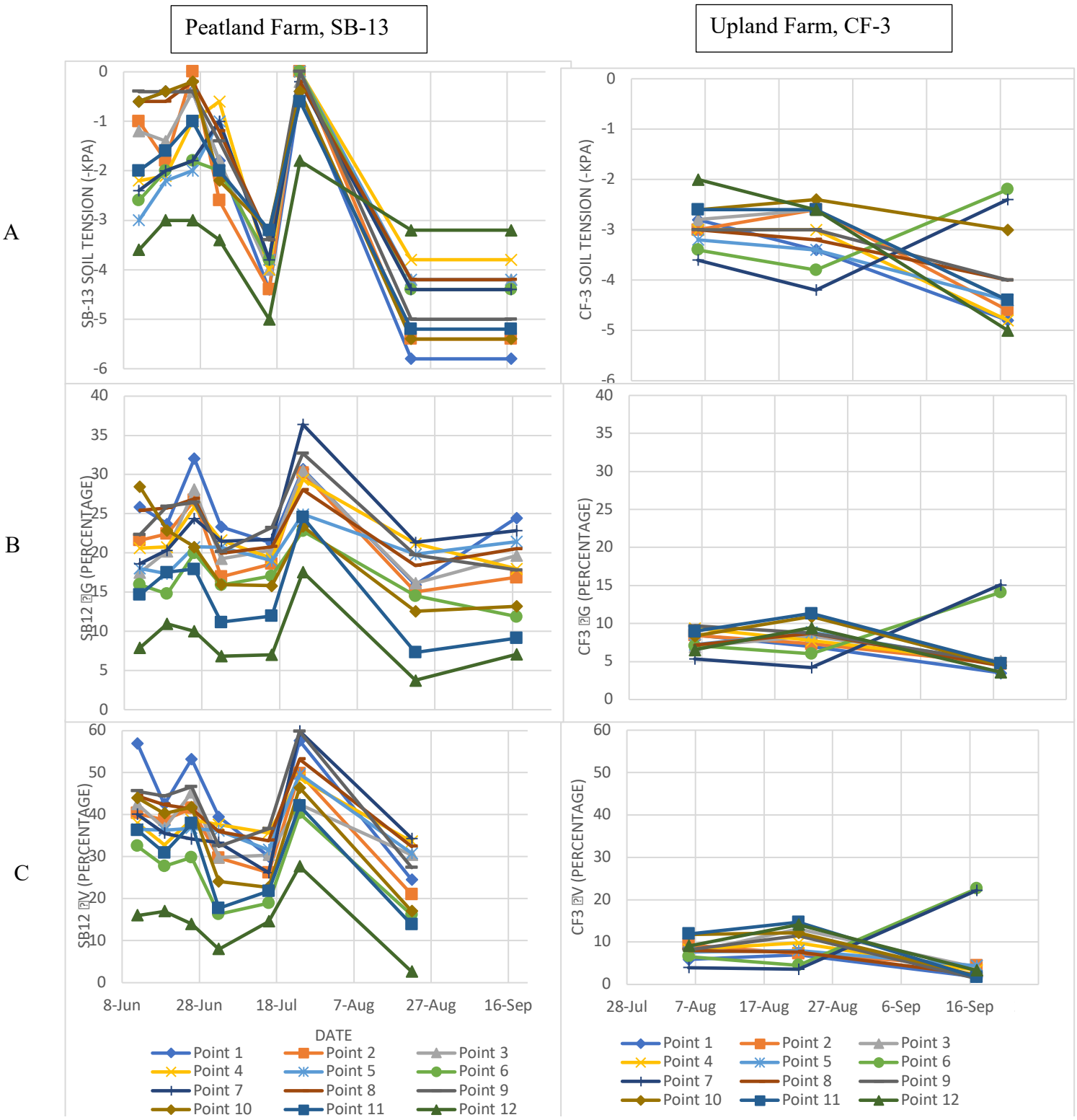

Figure 9: Point measurements were carried out at site SB (East Wareham, MA), peatland farm, and site CF (Carver, MA), upland farm, labeled by location and age of vines. SB-13 point measurements were collected between June 12, 2019, and Sep. 17, 2019. CF-3 point measurements were collected between Aug. 6, 2019 and Sep. 17, 2019. Panel A displays soil tension (ψ). Panel B displays gravimetric water content (θ_g). Panel C displays volumetric water content (θ_v). Twelve evenly distributed points were selected from each section. High ditches were observed at CF-3 on Sep. 17, 2019, where points 6 and 7 indicate a doubling of θ compared to the surrounding areas, potentially due to water encroachment from the ditches.

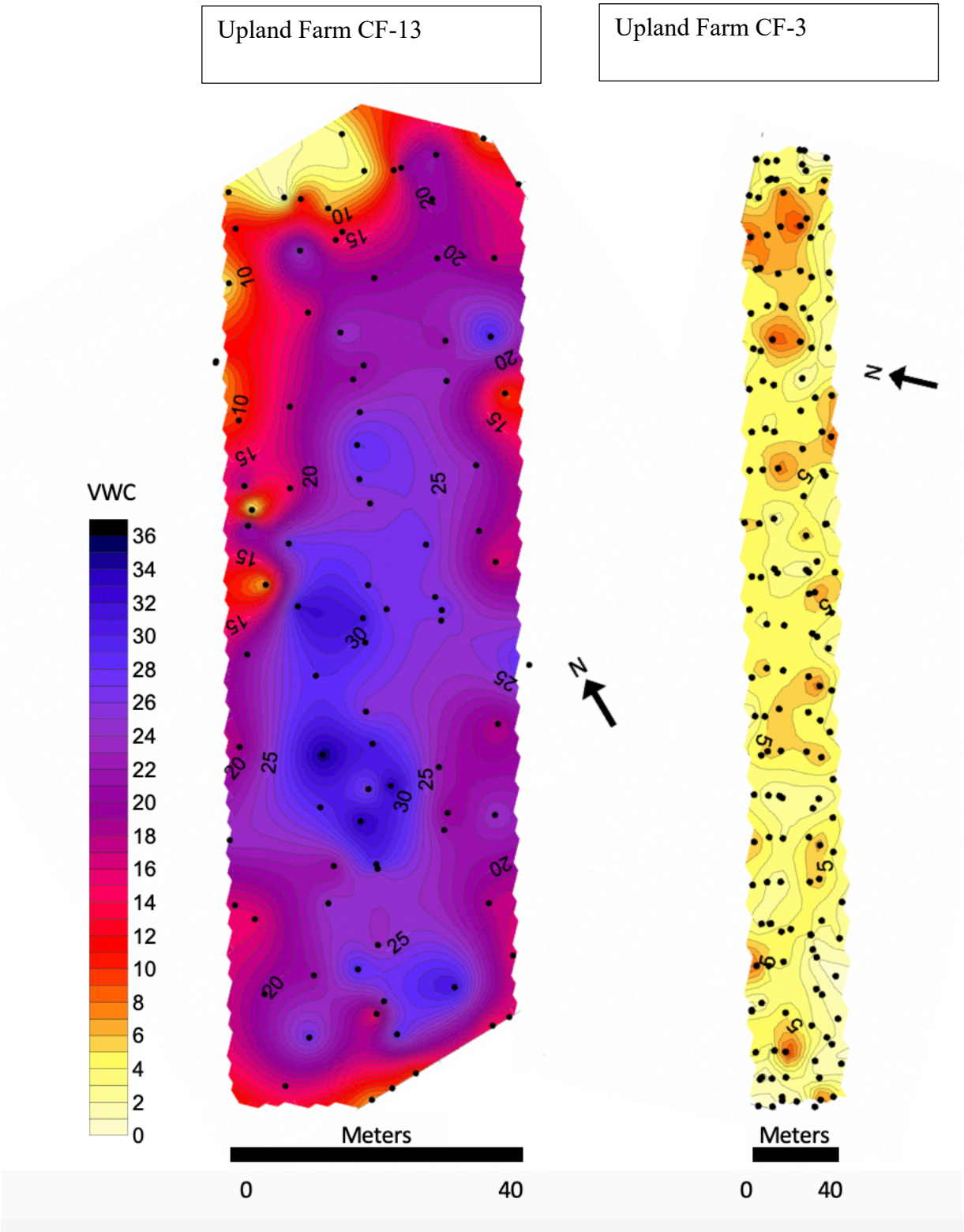

Figure 10: Maps of volumetric water content (θ_v) collected with TDR350 handheld probe (FieldScout; Spectrum Technologies) from SB-13 (East Wareham, MA), and CF-3 (Carver, MA) on Oct. 1, 2019. Maps consist of 150-200 point recordings.

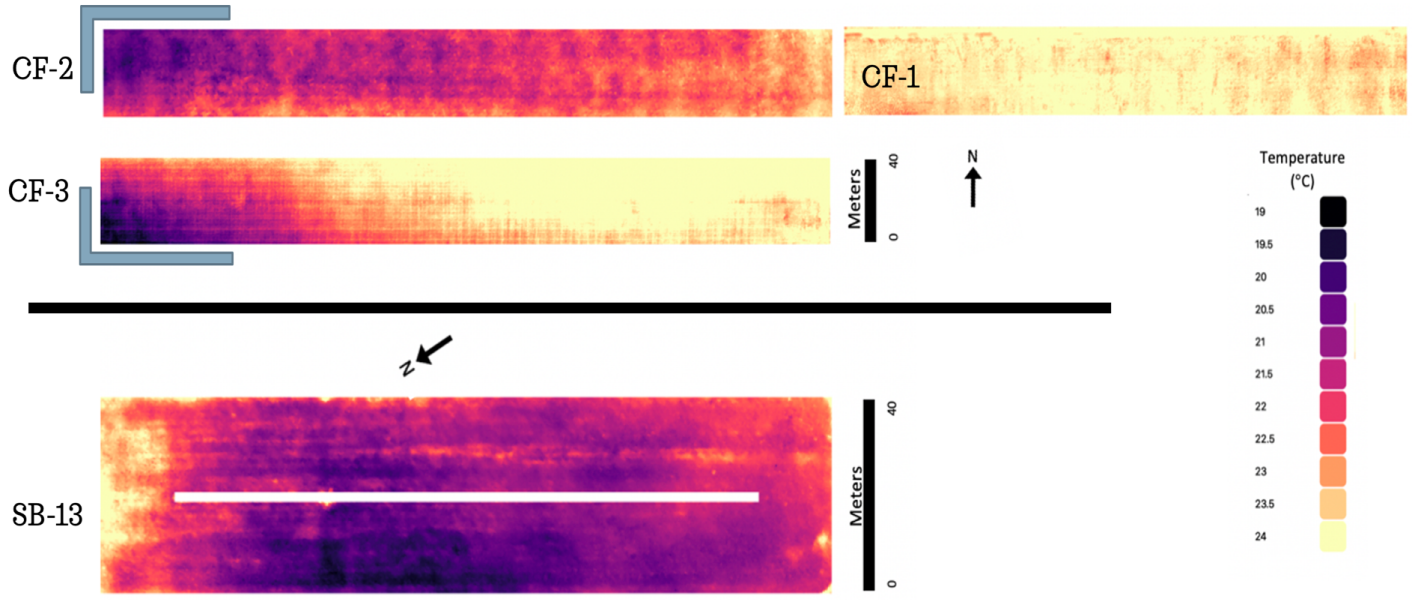

Figure 11. Infrared thermal orthomosaic images were collected from cranberry farms using a Zenmuse XT thermal camera (FLIR), on Aug. 5, 2019, between 9:30 PM and 11:00 PM. The temperature scale of the maps ranges from 19-24°C. SB-13 (East Wareham, MA) is cool in general, while CF-3 and CF-1 (Carver, MA) suggest cool conditions adjacent to canals with high water levels. Water levels within site CF canals were often raised overnight or early in the morning to provide subirrigation. This pattern of cooler/wetter soil near raised ditches was also seen on a Sep. 17, 2019 point collection.

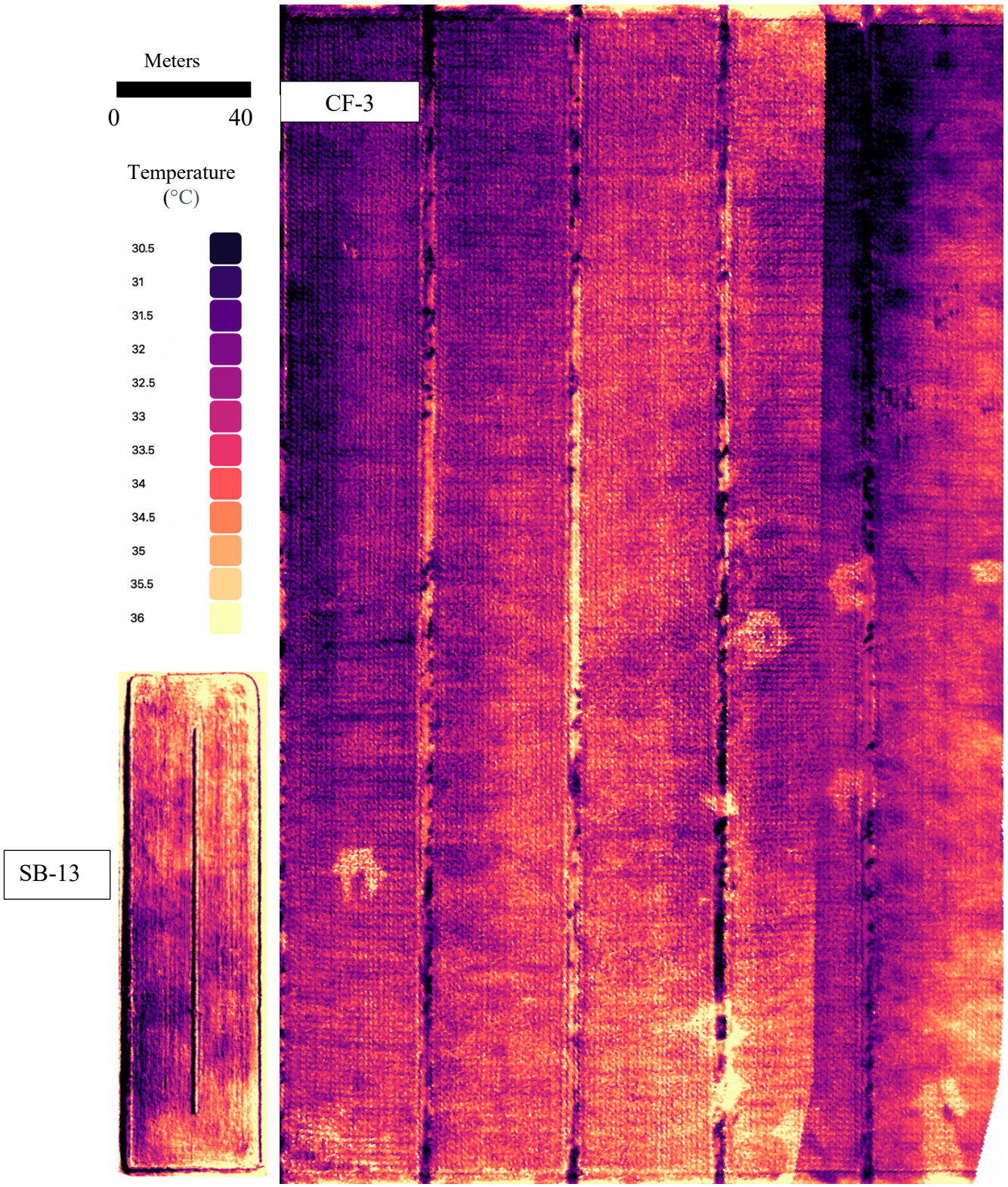

Figure 12: Daytime thermal images of SB-13 (East Wareham, MA) and CF-3 (Carver, MA), entire section, collected on Sep. 19, 2019. Flight was conducted using a Matrice 100 drone, flying at a height of 60 m and a speed of 8 m sec^{-1}. Images were collected using a Zenmuse XT (FLIR) thermal camera. During this flight, irrigation canals were filled with water (raised), depicted on the orthomosaic as cooler regions. CF-3 image experienced issues with stitching that resulted in temperature irregularities in the upper right corner (artificial cold coloration); however, hot spots suggesting irrigation failure are visible

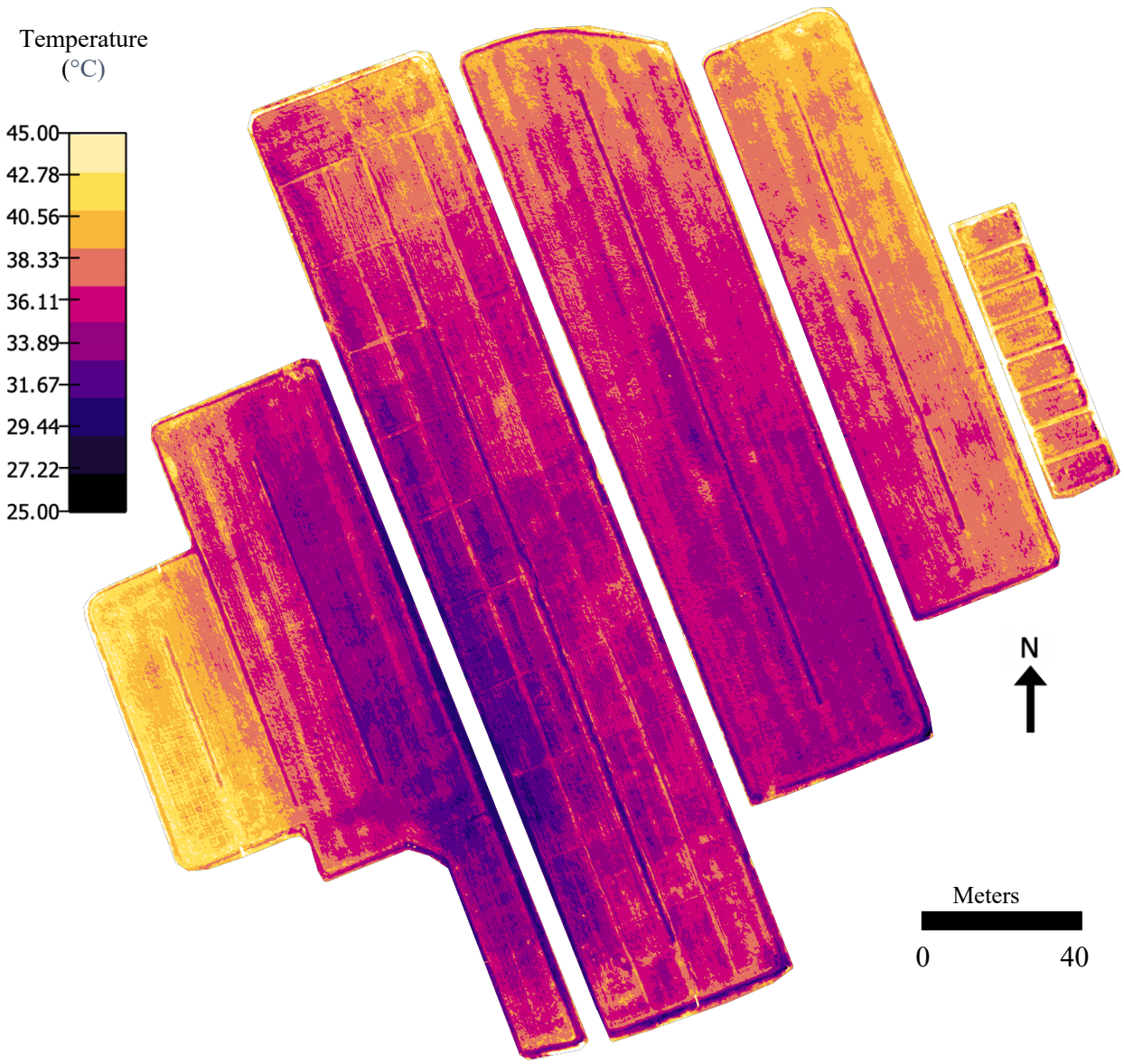

Figure 13: Thermal orthomosaic of site SB (East Wareham, MA), collected on July 16, 2019, during a daytime flight. Flight was conducted using the Matrice 100 drone, flying at a height of 60 m and a speed of 8 m sec^{-1}. Images were collected using a Zenmuse XT (FLIR) thermal camera. During this flight, irrigation canals were filled with water (raised), depicted on the orthomosaic as cooler regions.

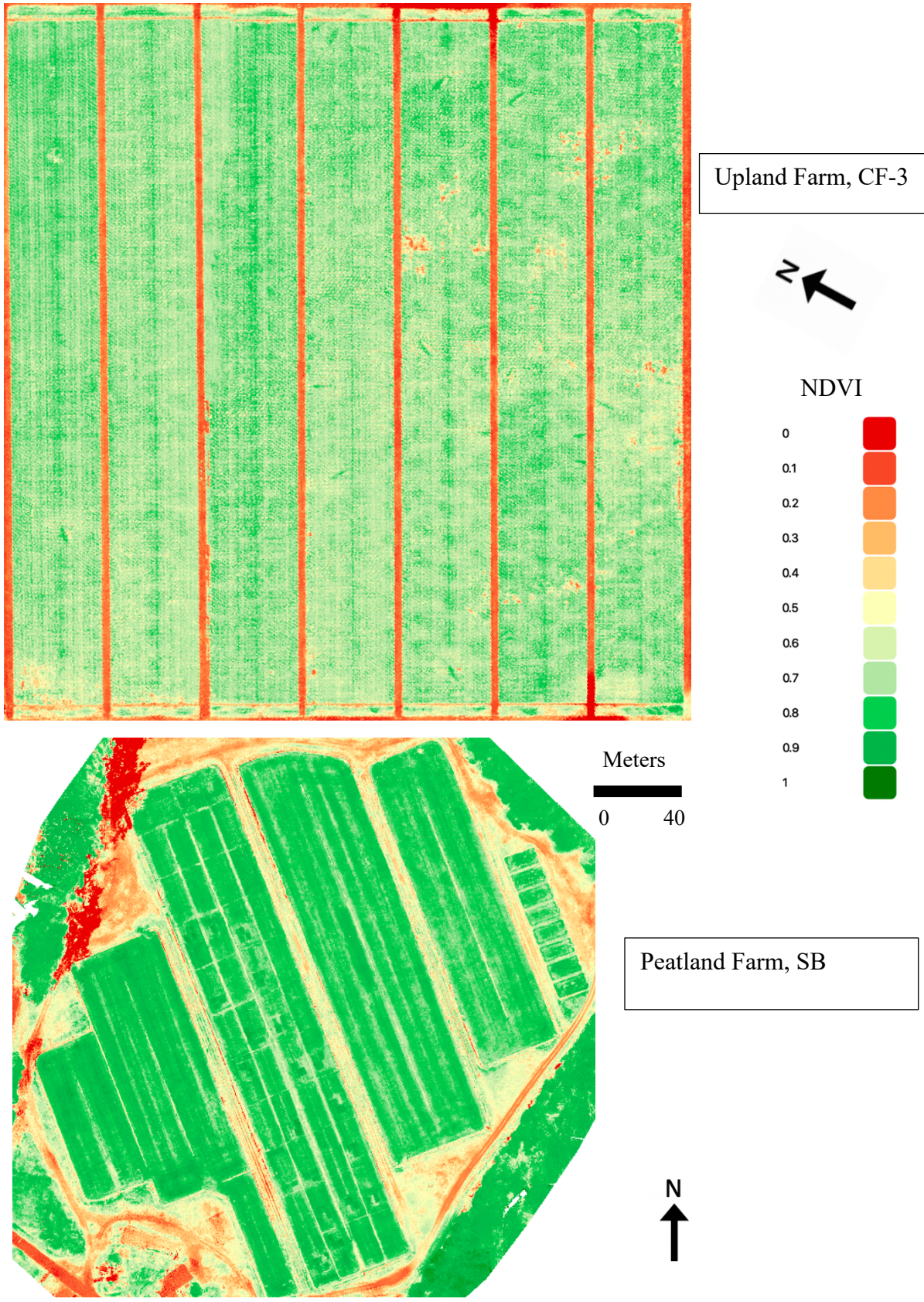

Figure 14: Normalized difference vegetation index (NDVI) images collected Sep. 17, 2019. Upper is CF-3 (Carver, MA), entire bog. Lower is site SB (East Wareham, MA). The rightmost section of site SB is SB-13. Overall, site SB has a higher NDVI than CF-3, given that vines are 13 yrs old and thoroughly established. CF-3 vines are 3 yrs old and much sparser than SB vines.

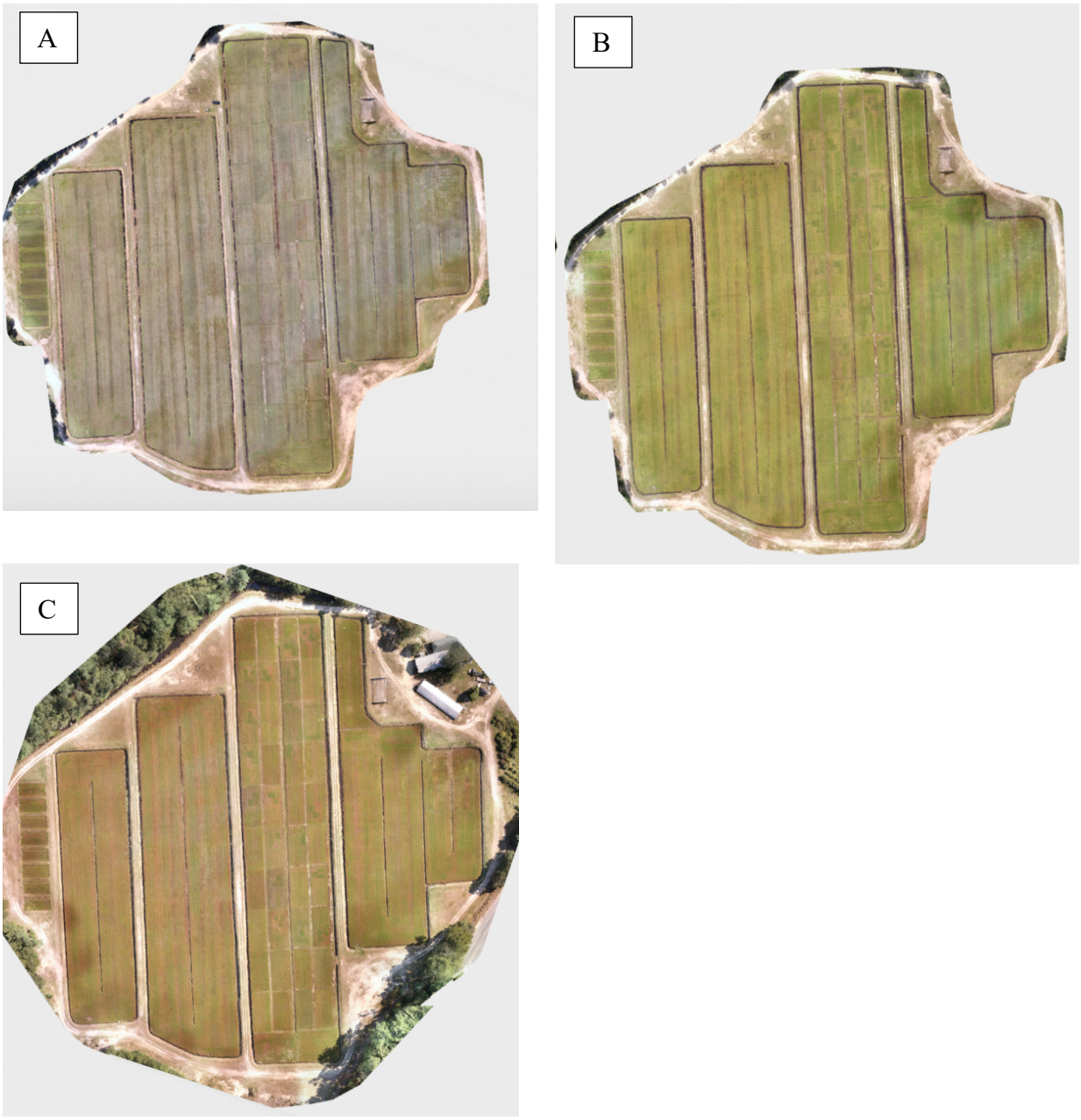

Figure 15: Stitched orthomosaic RGB images of site SB (East Wareham, MA). Images were collected using a Matrice 100 (DJI) drone and Parrot Sequoia (Micasense) multispectral camera. Panel A was collected on July 3, 2019, showing the farm during bloom, which gave the image a white cast. Panel B was collected on Aug. 1, 2019 and shows the farm during the part of the growing season when fruit were still green. Panel C, collected on Sep. 19, 2019 shows the farm one month before harvest, where the fruit have reached full size and have begun to turn red.

BIBLIOGRAPHY

Alston, J. M., Medellín-Azuara, J., Saitone, T. L. (2014). Economic Impact of the North American Cranberry Industry. https://www.uscranberries.com/wp-content/uploads/2018/09/Economic_Impact_of_the_NA_Cranberry_Industry_August2014-1.pdf. Accessed [2/13/20].

Baumann, D. L., Workmaster, B. A., Kosola, K. R. (2005). 'Ben Lear' and 'Stevens' cranberry root and shoot growth response to soil water potential. *HortScience*. 40: 795-798.

Bellvert, J., Zarco-Tejada, P. J., Girona, J., Fereres, E. (2014). Mapping crop water stress index in a 'Pinot-noir' vineyard: comparing ground measurements with thermal remote sensing imagery from an unmanned aerial vehicle. *Precis. Agric.* 15: 361-376.

Bilskie, J. (2001). Soil water status: content and potential. Campbell Scientific Publications. App. Note: 2S-I. https://s.campbellsci.com/documents/us/technical-papers/soilh20c.pdf Accessed [12/18/19].

Bland, W. L., Loew, J. T., Norman, J. M. (1995). Evaporation from cranberry. *Agric. For. Meteorol*. 81: 1-12.

Blatt, M. R., Chaumont, F., Farquhar, G. (2014). Focus on water. *Plant Phys*. 164: 1553-1555.

Bulot, D., Gumiere, S. J., Périard, Y., Lafond, J. A., Gallichand, J., Armaly-St-Gelais, M-H., Caron, J. (2016). Relationships among soil hydraulic properties, drainage efficiency, and cranberry yield. *Can. J. Soil Sci*. 97: 46-55.

Caron, J., Pelletier, V., Kennedy, C. D., Gallichand, J., Gumiere, S. Bonin, S., Bland, W. L., Pepin, S. (2017). Guidelines of irrigation and drainage management strategies to enhance cranberry production and optimize water use in North America. *Can. J. Soil Sci*. 97: 82-91.

Caruso, F.L. (1989). Phytophthora root rot of the cultivated cranberry in Massachusetts (*Vaccinium macrocarpon* Ait.). *Acta Hortic*. 241: 307-311

Caruso, F. (2008). "Cranberry Cultivars". p 72-80. In Sandler, H. A., DeMoranville, C. J. (eds.). Cranberry Production: A Guide for Massachusetts. University of Massachusetts, Amherst.

Cape Cod Cranberry Growers Association (CCCGA). (2019). The Cranberry: Where Tradition Meets Innovation. https://www.cranberries.org/history Accessed [01/15/20].

Chang, K-T. and Hsu, W-L. (2018). Estimating soil moisture content using unmanned aerial systems equipped with thermal infrared sensors. Institute of Electrical and Electronics Engineers International Symposium on Circuits and Systems. 1: 168-171.

Craft, C. (2016). "7- Peatlands". In: Creating and Restoring Wetlands: From theory to practice. *Elsevier Press, Amsterdam, NL*. 161-192 pp.

DeMoranville, C. J., Sandler, H. A., Caruso, F. L. (2001). Planting new cranberry beds: recommendations and management. UMass Extension Publication. http://www.umass.edu/cranberry/downloads/Planting%20New%20Cranberry%20Beds.pdf. Accessed [01/10/20].

DeMoranville, C. J., Kennedy, C. D., Jeranyama, P., Sandler, H. A., Saalau Rojas, E. (2016). Tile Drainage Best Management Practices. UMass Extension Publication. https://ag.umass.edu/sites/ag.umass.edu/files/pdf-doc-ppt/tile_drain_bmp_2016.pdf. Accessed [04/01/20].

Deubert, K. H., Caruso, F. L. (1989). Bogs and Cranberry Bogs in Southeastern Massachusetts. Massachusetts Agricultural Experiment Station. Research Bulletin Number 727. 35 pp.

De Vries, D. A. (1963). "Thermal properties of soils". In: W. R. van Wijk (ed.) Physics of plant environment. *North Holland Publishing. Amsterdam, NL*. 210-235 pp.

Eck, P. (1990). The American Cranberry. Rutgers University Press, New Brunswick, NJ. 420 pp.

Franklin, H. J. and Cross, C. E. (1948). Weather in relation to cranberry production and condition. Mass. Agr. Exp. Sta. Bul. 450. East Wareham, MA.

Engstrom-Heg, R. (1971). A Lightweight Mariotte Bottle for Field, Laboratory, and Hatchery Use. The Progressive Fish-Culturist, 33:4, 227-231, DOI: 10.1577/1548-8640(1971)33[227:ALMBFF]2.0.CO;2. Accessed [04/01/20].

Gago, J., Douthe, C., Coopman, R. E., Gallego, P. P., Ribos-Carbo, M., Flexas, J., Escalona, J., Medrano, H. (2015). UAVs challenge to assess water stress for sustainable agriculture. *Agric. Water Manag.* 153: 9-19.

Ghantous, K., Sylvia, M., Gauvin, D. (2018). Cranberry Chart Book 2018-2020; Management Guide for Massachusetts. University of Massachusetts Cranberry Station. https://ag.umass.edu/cranberry/publications-resources/cranberry-chart-book. Accessed [03/17/20].

Gleason, H.A. and Cronquist, A. (1991). Manual of Vascular Plants of Northeastern United States and Adjacent Canada. 2nd Edition, The New York Botanical Garden, Bronx, NY. http://dx.doi.org/10.21135/893273651.00. 910 pp.

Hare, D. K., Boutt, D. F., Clement, W. P., Hatch, C. E., Davenport, G., Hackman, A. (2017). "Hydrogeological controls on spatial patterns of groundwater discharge in peatlands". *Masters Theses*. University of Massachusetts-Amherst, Dept. of Geosciences. 93 pp.
https://scholarworks.umass.edu/masters_theses_2/152. Accessed [01/20/20].

Hattendorf, M. J. (1996). Cranberry evapotranspiration. *HortScience.* 31: 334-337.

Hoekstra, B. R., Neill, C., Kennedy, C. D. (2020). Trends in the Massachusetts cranberry industry create opportunities for the restoration of cultivated riparian wetlands. *Restor. Ecol.* 28: 185-195.

Hunsberger, L. K., DeMoranville, C. J., Autio, W.R., Sandler, H.A., (2006). Uniformity of sand deposition on cranberry farms and implications for swamp dodder control. *HortTechnology*. 16(3):488-492.

Ishimwe, R., Abutaleb, K., Ahmed, F. (2014). Applications of thermal imaging in agriculture- a review. *Adv. Remote Sens*. 3: 128-140.

Jackson T.J., Le Vine D. M., Swift C.T., Schmugge T.J., Schiebe F.R. (1995). Large area mapping of soil moisture using the ESTAR passive microwave radiometer in Washita'92. *Remote Sens. Environ*. 53: 27–37.

Jeranyama, P., DeMoranville, C. J., Kennedy, C. D. (2017). Evaluating tensiometers and moisture sensors for cranberry irrigation. *Acta Hortic.* 1180: 369-372.

Jones, H. G. (2004). Application of thermal imaging and infrared sensing in plant physiology and ecophysiology. *Adv. Bot. Res*. 41: 107-163.

Kay, B. D. and Goit, J. B. (1975). Temperature-dependent specific heats of dry soil materials. *Can. Geotech*. 12: 209-212.

Kennedy, C. D., Jeranyama, P., Alverson, N. (2017). Agricultural water requirements for commercial production of cranberries. *Can. J. Soil Sci*. 97: 38-45.

Kennedy, C. D., Wilderotter, S., Payne, M., Buda, A. R., Kleinman, P. J. A., Bryant, R. B. (2018). A geospatial model to quantify mean thickness of peat in cranberry bogs. *Geoderma*. 319: 122-131.

Kerry, R., Goovaerts, P., Giminez, D., Oudemans, P. V. (2017). Investigating temporal and spatial patterns of cranberry yield in New Jersey fields. *Precis. Agric*. 18: 507-524.

Kumundini, S. (2004). Effect of radiation and temperature on cranberry photosynthesis and characterization of diurnal change in photosynthesis *J. Am. Soc. Hortic. Sci*. 129: 106-111.

Lampinen, B. D. (2000). Construction, installation, and use of water level floats. UMass Extension Publication. http://www.umass.edu/cranberry/downloads/Water%20Level%20Floats.pdf. Accessed [01/10/20].

Laurent, T. (2014). Réponse de la canneberge (*Vaccinium macrocarpon* Ait.) à l'aération du sol. *Masters theses*, Université Laval, Québec, QC, Canada. 83 pp.

Neto C. C., Vinson J. A. (2011). "Cranberry". In: Benzie, I. F. F., Wachtel-Galor, S., (eds.). Herbal Medicine: Biomolecular and Clinical Aspects. 2nd edition. *Boca Raton FL: CRC Press/Taylor & Francis*. 107-130 pp.

Mallick, K., Bhattacharya, B. K., Patel, N. K. (2013). Estimating volumetric surface moisture content for cropped soils using a soil wetness index based on surface temperature and NDVI. *Agric. For. Meteorol*. 149: 1327-1342.

Masterson, J. P., Carlson, C. S., and Walter, D. A. (2009). Hydrogeology and simulation of groundwater flow in the Plymouth-Carver-Kingston-Duxbury aquifer system, southeastern Massachusetts, Scientific Investigations Report 2009–5063, 110 pp.

Mulla, D. J. (2013). Twenty-five years of remote sensing in precision agriculture: Key advances and remaining knowledge gaps. *Biosyst. Eng.* 114: 358-371.

Oudemans, P. V., Pozdnyakova, L., Hughes, M. G., Rahman, F. (2002). GIS and remote sensing for detecting yield loss in cranberry culture. *J. Nematol*. 34: 207-212.

Paredes-López, O., Cervantes-Ceja, M. L., Vigna-Pérez, M., Hernández-Pérez, T. (2010). Berries: improving human health and healthy aging and promoting quality life: A review. *Plant Foods Hum. Nutr*. 65: 299-308.

Pelletier, V., Gallichand, J., Caron, J., Justras, S., Marchand, S. (2015a). Critical irrigation threshold and cranberry yield components. *Agric. Water Manag*. 148: 106-112.

Pelletier, V., Gallichand, J., Gumiere, S., Pepin, S., Caron, J. (2015b). Water table control for increasing yield and saving water in cranberry production. *Sustainability* 7: 10602-10619.

Pelletier, V., Pepin, S., Gallichand, J., Caron, J. (2016a). Reducing cranberry heat stress and midday depression with evaporative cooling. *Sci. Hortic*. 19: 445-453.

Pelletier, V., Pepin, S., Laurent, T., Gallichand, J., and Caron, J. (2016b). Cranberry gas exchange under short-term hypoxic soil conditions. *HortScience*. 51: 910–914.

Pelletier, V., Gallichand, J., Gumiere, S., and Caron, J. (2017). Impact of drainage problems on cranberry yield: two case studies. *Can. J. Soil Sci*. 97: 1-4.

Robinson, D. A., Campbell, C. S., Hopmans, J. W., Hornbuckle, B. K., Jones, S. B., Knight, R, Ogden, F., Selker, J., Wendroth, O. (2008). Soil moisture measurement for ecological and hydrological watershed-scale observations: a review. *Vadose Zone J*. 7: 358-389.

Sandler, H., DeMoranville, C. J. (2008). Cranberry Production: A Guide for Massachusetts- Summary Edition. University of Massachusetts, Amherst. https://scholarworks.umass.edu/cgi/viewcontent.cgi?article=1000&context=cranberry_prod_guide. Accessed [09/10/19].

Sandler, H.A. (2009). Nitrogen rate, vine density, and weed management affect colonization of cranberry beds following disturbance-Preliminary observations. *Weed Technol*. 23: 324-328.

Sandler, H. A., Heywood, J. (Updated 2010). Sprinkler System Design and Use. UMass Extension Publications. https://ag.umass.edu/sites/ag.umass.edu/files/pdf-doc-ppt/bmp_sprinkler_system_design_and_use_2010.pdf. Accessed [11/10/19].

Sandler, H. A. (2018). Weed management in cranberries: a historical perspective and look to the future. *Agriculture*. 138: 1-20.

Santesteban, L. G., Di Gennaro, S. F., Herrero- Langreo, A., Miranda, C., Royo, J. B., Matese, A. (2017). High-resolution UAV-based thermal imaging to estimate the instantaneous and seasonal variability of plant water status within a vineyard. *AgricWater Manag*. 183: 49-59.

Saxton, K. E., Rawls, W.J. (2006). Soil water characteristics estimates by texture and organic matter for hydrologic solutions. *Soil Sci. Soc. Am. J*. 70: 1569-1578.

Shock, C. C., Wang, F-X. (2011). Soil water tension, a powerful measurement for production and stewardship. *HortScience*. 46: 178-185.

Smittle, D. A., Hall, M. R., Stansell, J. R. (1990). Irrigation regimes on yield and water use by sweetpotato. *J. Amer. Soc. Hortic. Sci*. 115: 712-714.

Soil Survey Staff, Natural Resources Conservation Service, United States Department of Agriculture. Web Soil Survey. Available online at the following link: https://websoilsurvey.sc.egov.usda.gov/. Accessed [09/10/19].

Thomas, J. D. (1990). Cranberry Harvest: A history of cranberry cultivation in Massachusetts. Spinner Publications, New Bedford, MA. 224 pp.

USDA National Agricultural Statistics Service. (2018). Massachusetts Cranberries. USDA National Agricultural Statistics Service. https://www.nass.usda.gov/StatisticsbyState/NewEnglandincludes/Publications/CurrentNews Release/2018/2017%20MA%20Cranberry%20Release_final.pdf. [Accessed 1/15/20].

Vanderleest, C. P. L., Bland, W. L. (2016). Evapotranspiration from cranberry compared with equilibrium rate. *Can. J. Soil Sci*. 97: 5-10.

Vanderleest, C. P. L., Caron, J., Bland, W. L. (2016). Water table level management as an irrigation strategy for cranberry (*Vaccinium macrocarpon* Aiton). *Can. J. Soil Sci*. 97: 11-19.

"Weather history for Wareham, MA for June 2019". *Weather underground*, The Weather Company. https://www.wunderground.com/history/daily/us/ma/wareham/KEWB. Accessed [1/7/20].

Zhang, D., Zhou, G, (2016). Estimation of soil moisture from optical and thermal remote sensing: a review. *Sensors*. 16: 1308-1337.

Zhang, C., Kovacs, J. M. (2012). The application of small unmanned aerial systems for precision agriculture: a review. *Precis. Agric*. 13: 693-712.

Zhang, J., Virk, S., Porter, W., Kenworthy, K., Sullivan, D., Schwarz, B. (2019). Applications of unmanned aerial vehicle based imagery in turfgrass field trials. *Front. Plant Sci*. 10:279. https://doi.org/10.3389/fpls.2019.00279.